Evolution of a Fault-Controlled, Deep-Water Sub-Basin, Tabernas, SE Spain

Lucie Baudouy [1,2*†‡], Peter D. W. Haughton [1‡] and John J. Walsh [2‡]

[1]UCD School of Earth Sciences, University College Dublin, Dublin, Ireland, [2]Fault Analysis Group, UCD School of Earth Sciences, University College Dublin, Dublin, Ireland

The Neogene Tabernas Basin, SE Spain, provides important evidence at outcrop for the interplay between tectonic deformation of the sea floor, slope instability and turbidity current behaviour. Dextral-oblique strike-slip faults and associated folds propagated along the basin axis to deform the palaeo-sea floor, creating structurally-controlled depressions in which turbidity currents were trapped and ponded. EW-trending syn-depositional faults define a narrow sub-basin that subsided asymmetrically as a negative flower structure. The sub-basin contains an expanded succession (>300 m of ponded turbidite sheets, debrites and slumps) along its northern margin flanked by the principal fault strand defined by a wide zone of sheared and calcite-veined marl. A narrower fault zone with a smaller displacement marks the southern margin of the sub-basin and the fill close to it is thin with internal discordances, evidence of local failure and southward thinning of sandstone sheets. Both northern and southern faults 'died' at the same stratigraphic level and were overstepped by basin floor turbidites showing evidence of weaker and longer-range topographic confinement. As turbidites healed and aggraded out of the sub-basin to progressively onlap the southern margin of the basin, major gravity failures occurred emplacing thick (>100 m) mass-transport complexes. The first initially reworked the southern part of the sub-basin fill together with the early onlap wedge, the second remobilised the onlap wedge, and the third records failure of the upper part of the slope well above the wedge. The first two were toe-confined failures, the third and furthest travelled was confined by basin axis topography. All three failures are lateral to or directly overlain by 'megabed' sheets on the basin floor, implying either a common trigger (earthquakes) or slope instability following reflection of large volume flows. Tabernas turbidites highlight the role of basin tectonics (as opposed to up-dip supply and sea level fluctuations) in directly impacting on deep-water processes and stratigraphy. Small deep-water transtensional sub-basins opened up along long transfer faults accommodating regional extension.

Keywords: ponded turbidites, mass-transport deposits, syn-depositional faulting, strike-slip faulting, negative flower structure

1 INTRODUCTION

Turbidity currents are extremely sensitive to slope (Britter and Linden, 1980; Kneller, 2003; Gray et al., 2005; Stevenson et al., 2013; Pohl et al., 2020) and respond to even subtle gradient changes induced by tectonic tilting or surface fault ruptures. Understanding the link between sea-floor deformation and sedimentation in deep-water successions has lagged behind that of more accessible fault-controlled terrestrial and shallow-water deposits. However, much recent progress has been made using seismic and bathymetric data from deforming continental slopes that demonstrate local flow ponding, transitions between channels and splays, and changes in channel sinuosity or position related to gradient breaks or lateral tilting (e.g. Pirmez et al., 2000; Heiniö and Davies, 2007; Caterall et al., 2010; Mayall et al., 2010; Doughty-Jones et al., 2017; Howlett et al., 2021; Pizzi et al., 2021). Nonetheless outcrop examples where tectonic control of sea floor gradients can be demonstrated are rare. Amongst those described are tectonically-forced lateral migration of channels and fans in the Ainsa Basin, northern Spain (Pickering and Corregidor, 2005; Tek et al., 2020), flow stripping across an emergent fault-scarp in the Annot Basin (Tomasso and Sinclair 2004), sandy lobes aggrading behind thrust-related folds in a trench slope setting on the Hikurangi Margin (McArthur et al., 2021), changes in bed type related to tectonic evolution of the Apennines foredeep (Tinterri and Muzzi Magalhaes, 2011; Tinterri and Piazza, 2019) and evidence for faulting on the floor of late Miocene basins in SE Spain (Haughton, 2000; Hodgson and Haughton, 2004). The study reported here builds on the first recognition of an important intrabasinal fault zone traversing the floor of the southern Tabernas Basin, SE Spain (Haughton, 2000). Here we demonstrate that the fault zone was part of a larger negative flower structure comprising several linked fault strands. These opened local fault-bounded accommodation (the Alfaro sub-basin) on the floor of a wider basin. The turbidite successions within and flanking the sub-basin record the history of sub-basin deepening, filling and healing that accompanied fault propagation to the sea floor. A significant feature of the sub-basin fill is the interplay between ponded turbidites and large-scale mass transport deposits (MTDs), particularly during healing of the basin floor. This interplay between tectonics, sea floor morphology and gravity current behaviour provides useful insight into processes operating in slope mini-basins with mobile shale or salt substrates.

The aims of this paper are to: 1) provide an improved tectonostratigraphic framework for the evolution of the Tabernas Basin and the associated Alfaro sub-basin based on new field mapping; 2) document the impact and displacement history of intrabasinal faults and show that these were part of a linked system sealed by the younger basin fill, 3) describe the pattern of sub-basin filling and healing as deformation transferred from intrabasinal faults to the basin margins, and 4) present evidence for onlap-wedge instability and the interplay between mass transport and turbidite systems as the structurally-generated topography was progressively buried. Evidence for the behaviour of syn-depositional faults sealed by younger stratigraphy is important regionally as it helps resolve the rapidly evolving Neogene deformation conditions in SE Spain.
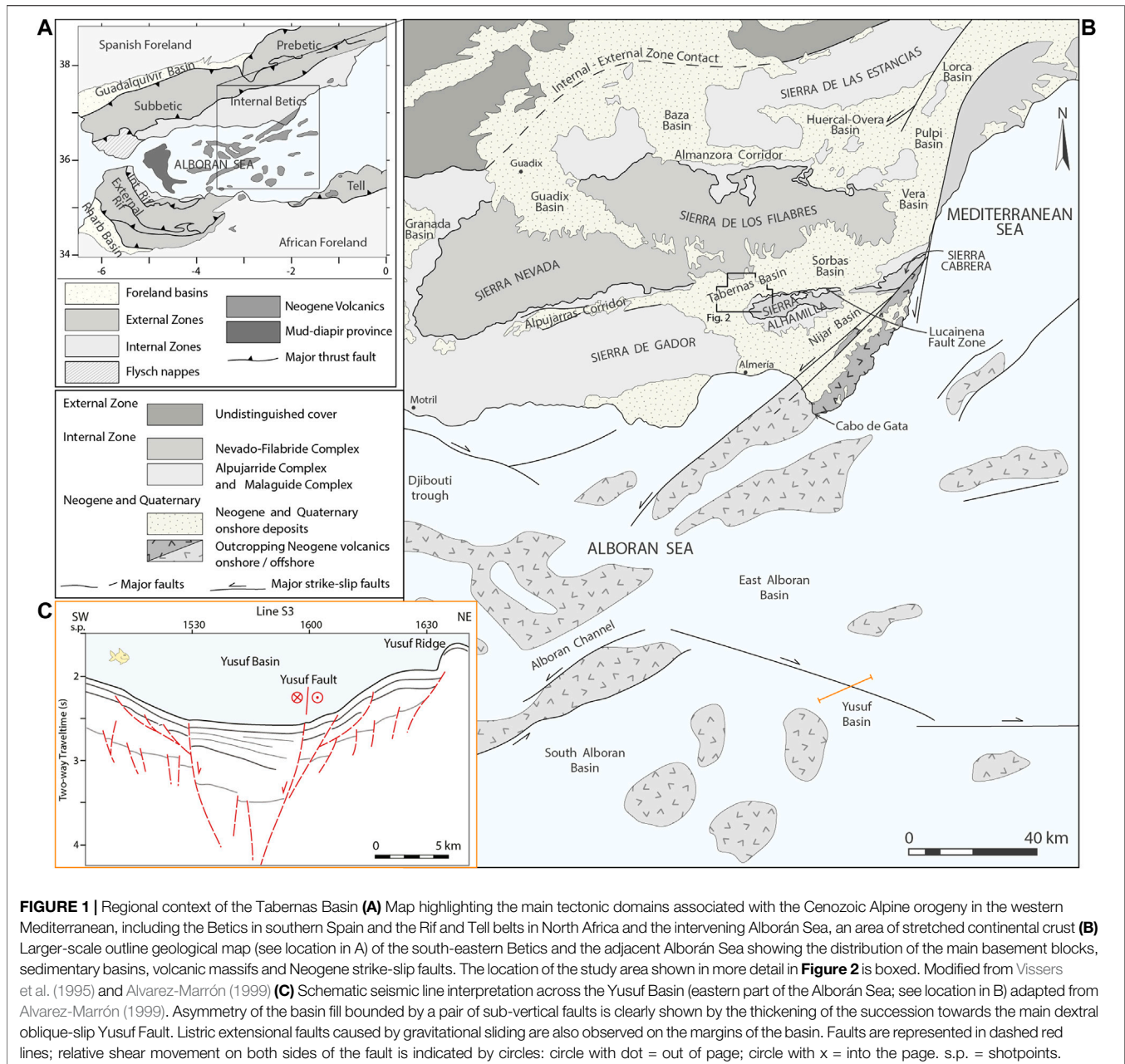
2 GEOLOGICAL SETTING

A network of small Neogene basins occurs throughout SE Spain and extends offshore into the Alboran Sea (**Figure 1**). The basins rest on exhumed basement rocks of the Internal Zone of the Betic Cordillera, the westernmost extension of the Alpine orogenic system (Lonergan and White 1997; Platt et al., 2013). The Tabernas Basin is typical of Neogene basins in the region in that it was a relatively narrow basin (~10 km wide, allowing for later compression) and elongated in an East-West direction. It is particularly well known for its deep-water fill first described by Kleverlaan (1989a,b). It was connected to the east with the Sorbas Basin and to the south with the Almería Basin (**Figure 1**), although each of the basins is characterised by a different subsidence pattern, fill, inversion and uplift history. The uplifted remnants of the Tabernas Basin are surrounded by basement cored mountains or sierras: the Sierra de los Filabres to the north composed mainly of high-grade metamorphic rocks (mainly dark mica-schist, gneiss and quartzite) assigned to the Nevado-Filabride Complex, and the Sierra Alhamilla and Sierra de Gádor to the south and south-west, respectively, which are dominated at surface by mainly lower-grade metamorphic rocks of the Alpujarride Complex (generally phyllites, psammites and dolomites). These basement highs and their extension to the west thus contributed compositionally distinct sediment to the adjacent basins (Koch and McCann 2020). Contemporary platform and pelagic carbonate production was also important, resulting in common mixed siliciclastic-carbonate sediment supply, as well as recycling of older Neogene basin fills.

3 TABERNAS BASIN

Kleverlaan (1989b) published the first detailed map and cross-sections of the Tabernas Basin fill. These illustrated the broad distribution of turbidite facies and highlighted the basin-wide distribution of a distinctive marker bed, a very thick (+ 60 m) debrite-turbidite couplet which was termed the Gordo Megabed (Kleverlaan 1987). Haughton (2000) subsequently provided a revised map for part of the southern section of the basin tracing distinctive stacked turbidite units assigned formation status in Hodgson and Haughton (2004). Since then, remapping has focussed on better integrating stratigraphic and structural aspects of the basin fill, and in particular in distinguishing syn and post-depositional faults. The result is the new map and cross-sections shown in **Figures 2**, **3**.

The Tabernas Basin fill rests unconformably on the Sierra de los Filabres basement to the north and is up-ended and faulted against the Sierra Alhamilla basement in the south-east. The latter faulted contact is the westward extension of the Lucainena Fault Zone (Galdeano and Vera, 1992) that runs along the northern flank of the Sierra Alhamilla for over 35 km. East of

FIGURE 1 | Regional context of the Tabernas Basin **(A)** Map highlighting the main tectonic domains associated with the Cenozoic Alpine orogeny in the western Mediterranean, including the Betics in southern Spain and the Rif and Tell belts in North Africa and the intervening Alborán Sea, an area of stretched continental crust **(B)** Larger-scale outline geological map (see location in A) of the south-eastern Betics and the adjacent Alborán Sea showing the distribution of the main basement blocks, sedimentary basins, volcanic massifs and Neogene strike-slip faults. The location of the study area shown in more detail in **Figure 2** is boxed. Modified from Vissers et al. (1995) and Alvarez-Marrón (1999) **(C)** Schematic seismic line interpretation across the Yusuf Basin (eastern part of the Alborán Sea; see location in B) adapted from Alvarez-Marrón (1999). Asymmetry of the basin fill bounded by a pair of sub-vertical faults is clearly shown by the thickening of the succession towards the main dextral oblique-slip Yusuf Fault. Listric extensional faults caused by gravitational sliding are also observed on the margins of the basin. Faults are represented in dashed red lines; relative shear movement on both sides of the fault is indicated by circles: circle with dot = out of page; circle with x = into the page. s.p. = shotpoints.
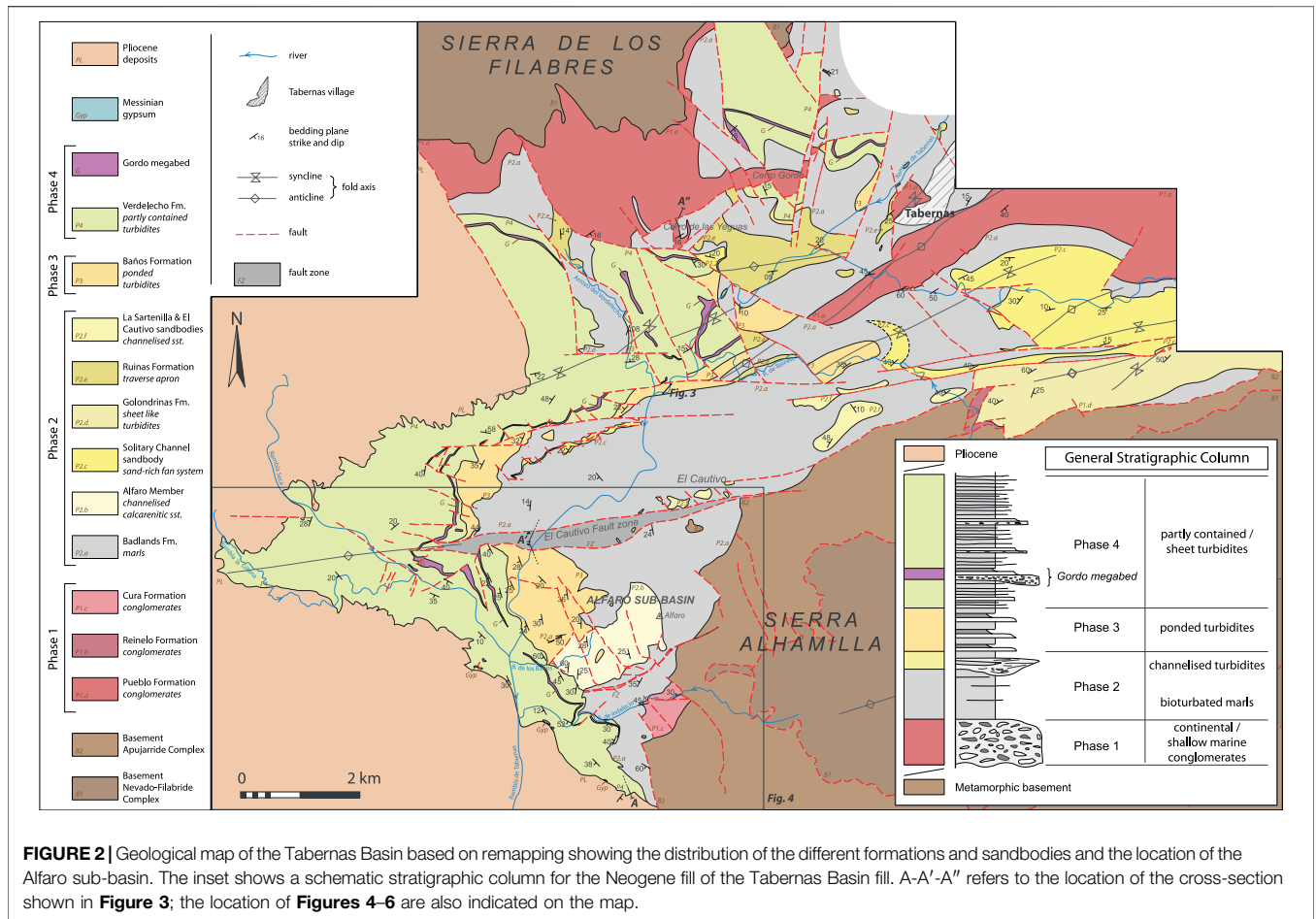
Lucainena, the Lucainena Fault Zone is unconformably overstepped by latest Tortonian-Messinian reefs and associated shallow marine deposits (Weijermars et al., 1985; Martín et al., 1998; Haughton, 2001). At the western plunge culmination of the Sierra Alhamilla, the fault propagates westwards up-dip into the Tabernas basin fill as the El Cautivo Fault Zone—but again it is overstepped by younger stratigraphy implying that it became inactive in the early Messininan. It is an area of stratigraphic expansion directly south of the El Cautivo Fault, here referred to as the Alfaro sub-basin, that is the subject of this paper. To the west, the deep-water fill to the Tabernas Basin is blanketed unconformably by younger Pliocene deposits locally affected by NNW-SSE

trending normal faults and E-W strike-slip faults (Sanz De Galdeano et al., 2010). To the east, it passes axially into the Sorbas Basin fill, although the Tabernas Basin remained a deep water basin at the end of the Tortonian whereas the Sorbas Basin was uplifted, eroded and became a shallower water platform.

Mapping of the Tabernas Basin fill reveals four distinct phases in basin development (**Figure 2**); these represent significant structurally-driven reconfigurations of the basin shape and sediment supply.

Phase 1 comprises an upward-fining succession of very coarse boulder conglomerates passing upwards into yellow-grey marine marls. The conglomerates rest unconformably on metamorphic basement along the foot of the Sierra de los Filabres, and are
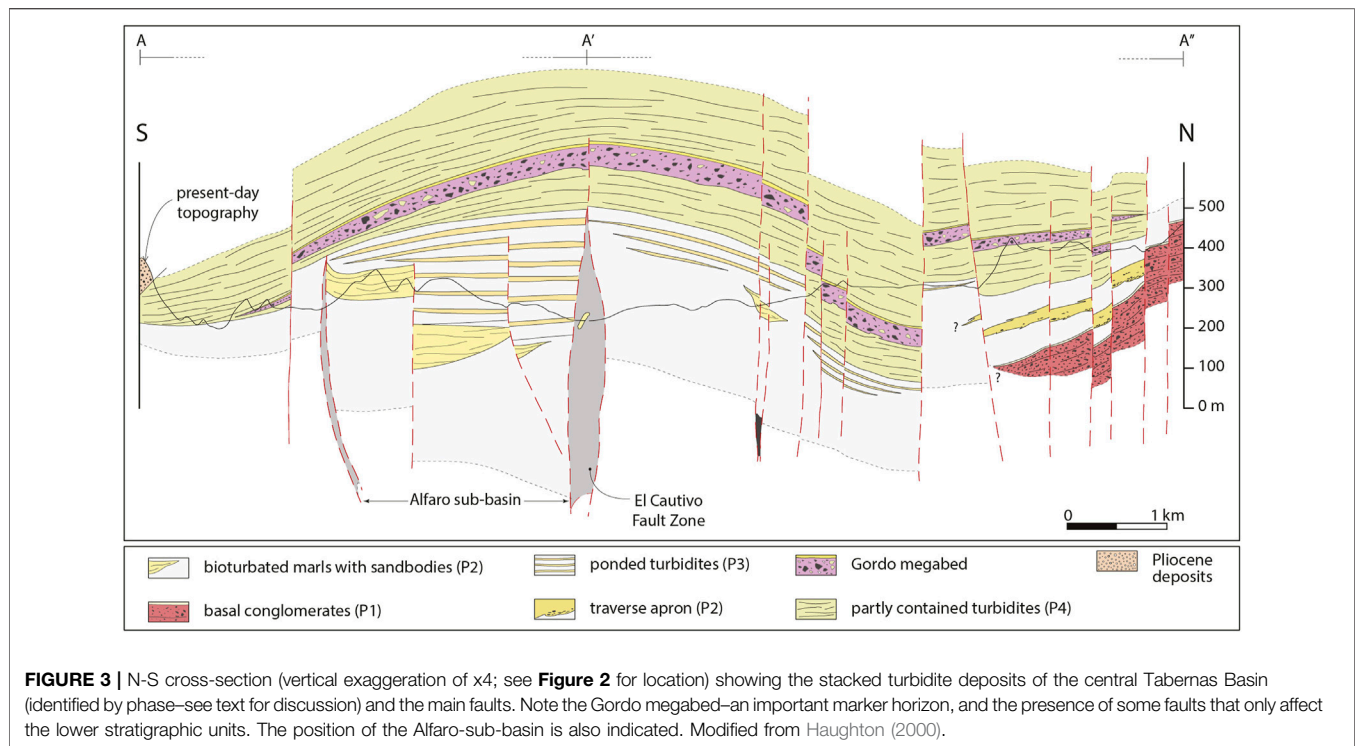
FIGURE 2 | Geological map of the Tabernas Basin based on remapping showing the distribution of the different formations and sandbodies and the location of the Alfaro sub-basin. The inset shows a schematic stratigraphic column for the Neogene fill of the Tabernas Basin fill. A-A′-A″ refers to the location of the cross-section shown in **Figure 3**; the location of **Figures 4–6** are also indicated on the map.

brought to the surface in a pair of faulted anticlines at Cerro Gordo and south of Tabernas (**Figure 2**). The conglomerates record the early deposition of terrestrial alluvial fans that evolved to become fan deltas as a consequence of marine flooding (Dabrio, 1990; Doyle et al., 1996). This earlier phase of basin development is poorly dated but a Serravallian to early/mid Tortonian age has been inferred (Kleverlaan, 1987, 1989a; Poisson et al., 1999; Hodgson, 2002). Sediment dispersal was to the south and south-west from a source mainly comprising Nevado-Filabride basement lithologies (graphic schist and psammite). The conglomerates (several 100 m thick) may be related to Alpujarride-sourced conglomerates passing up into yellow-grey marls found in normal fault-contact with the Sierra Alhamilla east of Alfaro hill, and caught up as slivers in the fault zone juxtaposing the basin and basement along the north side of the Alhamilla (where they are locally unconformable on the Alpujarride basement and overstepped by younger late Tortonian turbidites). The early upward-fining successions may be remnants of the hanging-wall fill to extensional detachments formed during the later stages of an extensional event that regionally thinned the basement (Martínez-Martínez and Azañón, 1997; Martínez-Martínez and Azañón, 2002; Giaconia et al., 2014). This is consistent

with clast imbrication and grain size and facies trends suggesting flow to the SW (e.g. at Cerro Gordo west of Tabernas; **Figure 2**).

Phase 2 post-dates regional extension and was characterised by the development of an EW elongate depocentre in which a thick succession (>200 m) of late Tortonian grey marls initially accumulated in the basin axis, thinning onto the flanks of the basin. Towards the top of Phase 2, coarse grained sediment advanced into the basin, initially as northerly-derived, poorly sorted conglomerates and breccias interpreted as a deep-water apron related to reactivation of the northern basin margin (**Figure 3**). More mature W-derived conglomerates and sandstones filled a number of large axial slope channel fills in the basin axis and locally overlie the transverse apron south of the Cerro de las Yeguas (**Figure 2**). These were described by Haughton (2000) and interpreted as backfilled channels traversing an east-facing axial slope—they probably fed basin floor fans in the eastern Tabernas basin at this time and tapped a variable mix of Nevado-Filabride and Alpujarrdide sourced sediment supplied from the west.

Phase 3 represents a muddy phase of basin filling with the axial slope replaced by an uneven but relatively flat basin floor with depressions in which fully-contained (sensu Pickering and Hiscott, 1985) sheet turbidites accumulated. The term sheet is used here to

FIGURE 3 | N-S cross-section (vertical exaggeration of x4; see **Figure 2** for location) showing the stacked turbidite deposits of the central Tabernas Basin (identified by phase–see text for discussion) and the main faults. Note the Gordo megabed–an important marker horizon, and the presence of some faults that only affect the lower stratigraphic units. The position of the Alfaro-sub-basin is also indicated. Modified from Haughton (2000).

refer to laterally extensive single beds that extend across the area with minimal variation in thickness and which are limited by onlap onto topography or truncation against syn-depositional faults. Deposition was thus focussed across areas of deeper bathymetry; the sheets thin onto the basin margins and over intrabasinal highs (**Figure 2** and **Figure 3**). Turbidity currents were derived from the west with no evidence for sediment dispersed from the northern basin margin at this time; evidence for ponding of the flows implies there was now no exit for flows to the east and this probably corresponds to uplift of the southern part of the Sorbas Basin in the latest Tortonian/early Messininan.

Phase 4 (Messinian) saw a return to northerly-derived sediment following rejuvenation and uplift of the Filabres source; both transverse and larger volume axial turbidity currents spread sand across the basin floor, blanketing early intrabasinal structures, and onlapping unstable slopes on the south side of the basin. Phase 4 also saw the introduction of a series of megabeds, most spectacular of which was the Gordo Megabed of Kleverlaan (1987). The latter provides a useful datum for correlating stratigraphy across the basin. We distinguish here between megabeds, basin-wide large volume event beds comprising a basal breccia (debrite) overlain by a central sandstone grading upwards into a upper thick mudstone cap (a contained turbidite), and mass transport deposits, less well-organised and laterally more restricted products of slope failure involving slumping, sliding and local transformation to a debris flow.
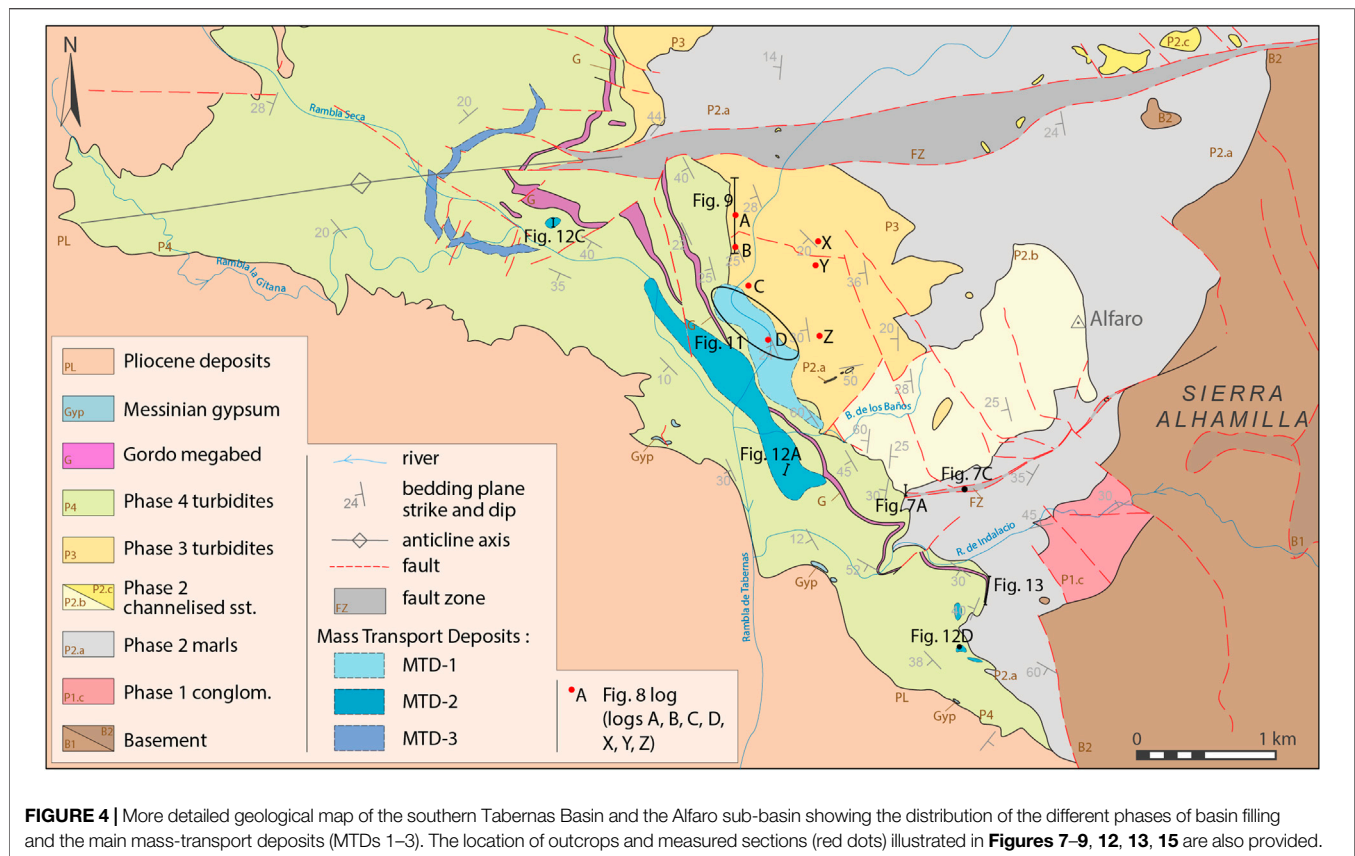
The focus of this paper is on understanding phases 2, 3 and 4 of basin evolution in the area south of the El Cautivo Fault Zone in the southern part of the Tabernas Basin where an anomalously thick Phase 3 succession is preserved within the Alfaro sub-basin (**Figure 3**). The following sections first describe the margins of the sub-basin, concentrating on the southern margin which has not

been described before, and then analysing the fill and the relationship of the turbidite stratigraphy to early faults.

4 ALFARO SUB-BASIN

The Alfaro sub-basin fill is well exposed on the western flanks of Alfaro hill and in the Rambla de Tabernas (**Figure 4**). Its northern margin corresponds to the E-W trending El Cautivo Fault Zone described in detail by Hodgson and Haughton (2004). This dextral oblique soft-sediment shear zone is interpreted as a fault that propagated to the palaeo-sea floor through unconsolidated marl on account of its width (up to 350 m of muddy gouge including disrupted blocks of Phase 2 turbidite sand/sandstone), flared geometry and significant thickening of the Phase 3 'contained turbidite' succession across it. The fault zone is characterised by a complex array of syn-kinematic fibrous calcite veins implying significant fluid movement during fault activity.

The succession immediately south of the El Cautivo Fault can be linked to that to the north, albeit with some important differences. Locally-derived basal conglomerates (up to 25 m thick) with an Alpujarride provenance and bioclastic components occur in normal-fault contact with Alpujarride basement. Hodgson (2002) has argued that these conglomerates contain evidence for syn-depositional NE-SW extension. They are overlain by yellow-grey marls with rare thin calcarenitic sandstone sheets that are well seen on the eastern counter-dip slopes of Alfaro hill. This fining upward conglomerate succession is tentatively assigned to Phase 1 (i.e. the early extensional phase of basin evolution), although it may not be age-equivalent to Phase 1 in the northern Tabernas Basin. However the

FIGURE 4 | More detailed geological map of the southern Tabernas Basin and the Alfaro sub-basin showing the distribution of the different phases of basin filling and the main mass-transport deposits (MTDs 1–3). The location of outcrops and measured sections (red dots) illustrated in **Figures 7–9**, **12**, **13**, **15** are also provided.

thick muddy succession overlying the conglomerates is similar to the Phase 2 marls observed in the northern part of the basin.
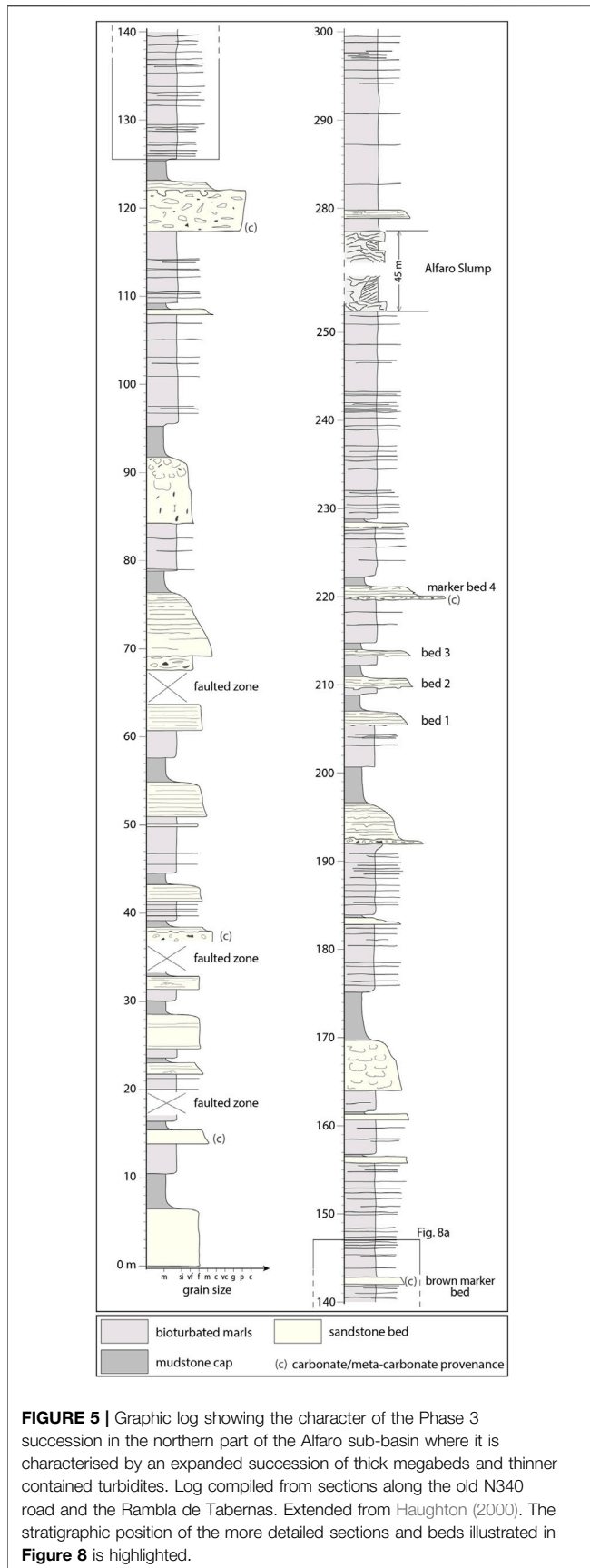
A sharp erosional contact just beneath the crest of Alfaro hill separates the marls from an overlying stack of calcarenitic sandstones and microconglomerates (up to 70 m thick, Alfaro Member of Iaccarino et al., 1975). The calcarenites are rich in dolomite pebbles and contemporary bioclastic components and form two sandy packages separated by a 5 m thick discontinuous marl interval. Pebble imbrication indicates transport to the east. The calcarenites pass gradationally upwards into marl. The Alfaro Member is interpreted as two or more nested Phase 2 axial slope channels on the basis of the erosional bases, coarse grain size, amalgamation of sandstone beds and transport to the east similar to other Phase 2 channels (Haughton, 2000; Pickering et al., 2001). The channel bodies are overlain by up to 300 m of marls with thick ponded sandstone sheets [Unit C of Haughton (2000)] which occur on the western dip slope of Alfaro hill and in high cliffs along the western side of the Rambla de Tabernas. The sandstone sheets are dominantly of schistose metamorphic provenance, although there are some interleaved calcarenitic units (debrite-turbidite couplets). Most thicker sandstone beds have unbioturbated, more fissile capping mudstone divisions that are as thick or thicker than the underlying sandstones. This is the local expanded expression of Phase 3 deposition within the sub-basin (**Figure 5**). On the west side of Rambla de Tabernas, the change from Phase 3 to Phase 4 basin fill is marked by a step-change in the sandstone bed thickness distribution, bed frequency

and bed structure (Haughton, 2000). Thin and very thin beds are rare in the Phase 3 ponded fill, whereas these are common in Phase 4 and there is an attendant change in overall colour from grey to brown as well as an increase in bed frequency.

4.1 Stratigraphic Relationship Across the Northern Sub-basin Margin

Evidence for stratigraphic changes across the northern sub-basin margin has been addressed by Hodgson and Haughton (2004). Phase 3 sheets abut directly against the El Cautivo Fault Zone (ECFZ) which juxtaposes the ponded turbidite sheets to the south against thick marls to the north. There is no evidence for significant thinning of the turbidite sheets before they are cut by the fault zone. Only a thin interval of Phase 3 sheets (30 m thick) occurs directly north of the ECFZ just beneath the transition to Phase 4 fill. These cannot be tied at a bed level to sheets within the sub-basin. The sandier Phase 4 succession steps across the fault with only minor (m scale) later displacement.

Unlike the sheet turbidites, the underlying Alfaro Member calcarenites do not extend off the crest of Alfaro hill northwards as far as the ECFZ. Nested channel surfaces step up to the north and the calcarenites pinch out approximately 1 km south of the fault trace. Calcarenitic beds are however caught up in the thick gouge zone associated with the EFCZ. Calcarenitic beds also locally cap hills on the north side of the fault zone and are interpreted to represent the erosional remnants of another Phase

FIGURE 5 | Graphic log showing the character of the Phase 3 succession in the northern part of the Alfaro sub-basin where it is characterised by an expanded succession of thick megabeds and thinner contained turbidites. Log compiled from sections along the old N340 road and the Rambla de Tabernas. Extended from Haughton (2000). The stratigraphic position of the more detailed sections and beds illustrated in **Figure 8** is highlighted.

2 channel system, this one filled with sand with a mixed carbonate-siliciclastic provenance. At El Cautivo (**Figure 2**), this channel appears to have been truncated by the ECFZ to which it is oblique at a low angle in plan view.

Interpretation: Phase 4 sandstones overstep the ECFZ yet the Phase 3 sheet turbidites are truncated by the fault, implying the fault was active during or at least towards the end of Phase 3 deposition and then became inactive or buried by an increase in the rate of sediment accumulation. The expansion of the Phase 3 stratigraphy across the fault implies either an element of growth and/or lateral displacement of a thicker against a thinner sheet turbidite succession. The Alfaro calcarenite-filled channels step towards the fault zone but are separated from it suggesting the fault did not directly control the channel location. The northward stepping of channels may reflect early tilting towards the fault. The obliquity between channel orientations and the fault trend also suggests the fault was largely post channel formation, as do the large blocks of calcarenite resembling channel sediment (some cemented) that float within the fault gouge zone. The blocks were presumably entrained where the faults propagated to displace the channel fills cutting across the fault trace.

4.2 Phase 3 Sheets North of the Alfaro Sub-basin

The Phase 3 ponded sheet succession thickens northwards away from the sub-basin, reaching 100 m thick c.2 km north of the El Cautivo Fault before the sandstones pinch out laterally again into marl in the Arroyo del Verdelecho (**Figure 2**). The same sheets can also be traced eastwards 2.5 km in the Rambla de Reinelo where the thickest bed reaches >5 m thick. In general, however, the event beds are thinner than their equivalents in the expanded sub-basin succession and thick mudstone caps are less well developed. The character of the sheets outside the sub-basin is well illustrated by a large exposure in the Rambla de Tabernas (just upstream of its junction with the Arroyo del Verdelecho; **Figure 6**). Here a sandstone-mudstone couplet is characterised by a parallel-laminated sandstone with local convolute folding of the lamination upstream of a thinned part of the bed. The sandstone component of the event bed varies from 80 to 200 cm due to an irregular base as it rests on up to 10 m of remobilised marl. The bed is displaced by a series of normal listric faults orientated N115E and dipping to the south. The faults root out at the base of the muddy slumped interval but do not extend to the upper part of the outcrop to cut the next sandstone sheet. The fault planes have locally been intruded by marl.

Interpretation: Gradual expansion and then thinning of the Phase 3 sheet succession northwards away from the El Cautivo Fault Zone suggests that ponding of turbidity took place in gentle depressions up to 2 km across and > 3 km long, as well as in the deeper fault-controlled bathymetry of the sub-basin. The thickest sheets encountered outside of the sub-basin are in the Rambla de Reinelo and coincide with the hinge of a syncline. It is possible therefore that the basin floor outside of the sub-basin was warped by contemporary folding, with turbidites deposited along developing synclinal axes. Some of the sandstones directly overlie cohesive mudflow deposits suggesting that they were
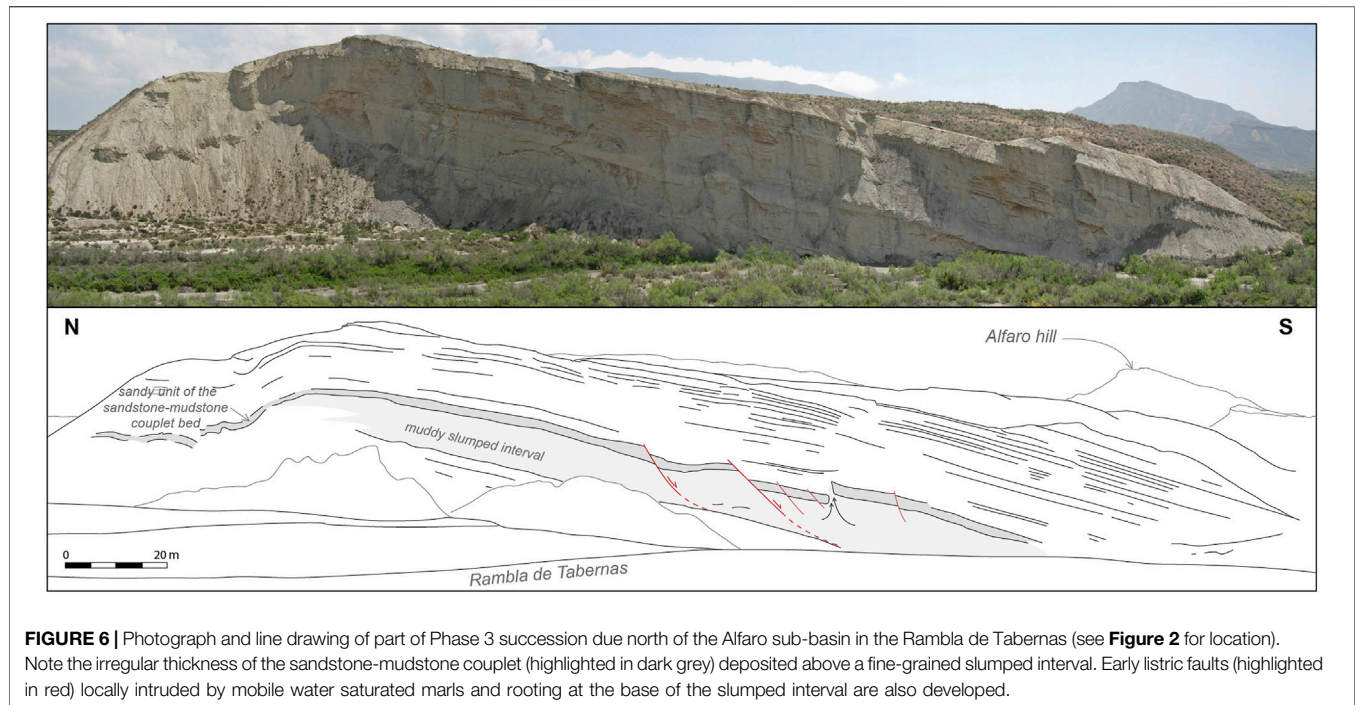
FIGURE 6 | Photograph and line drawing of part of Phase 3 succession due north of the Alfaro sub-basin in the Rambla de Tabernas (see **Figure 2** for location). Note the irregular thickness of the sandstone-mudstone couplet (highlighted in dark grey) deposited above a fine-grained slumped interval. Early listric faults (highlighted in red) locally intruded by mobile water saturated marls and rooting at the base of the slumped interval are also developed.
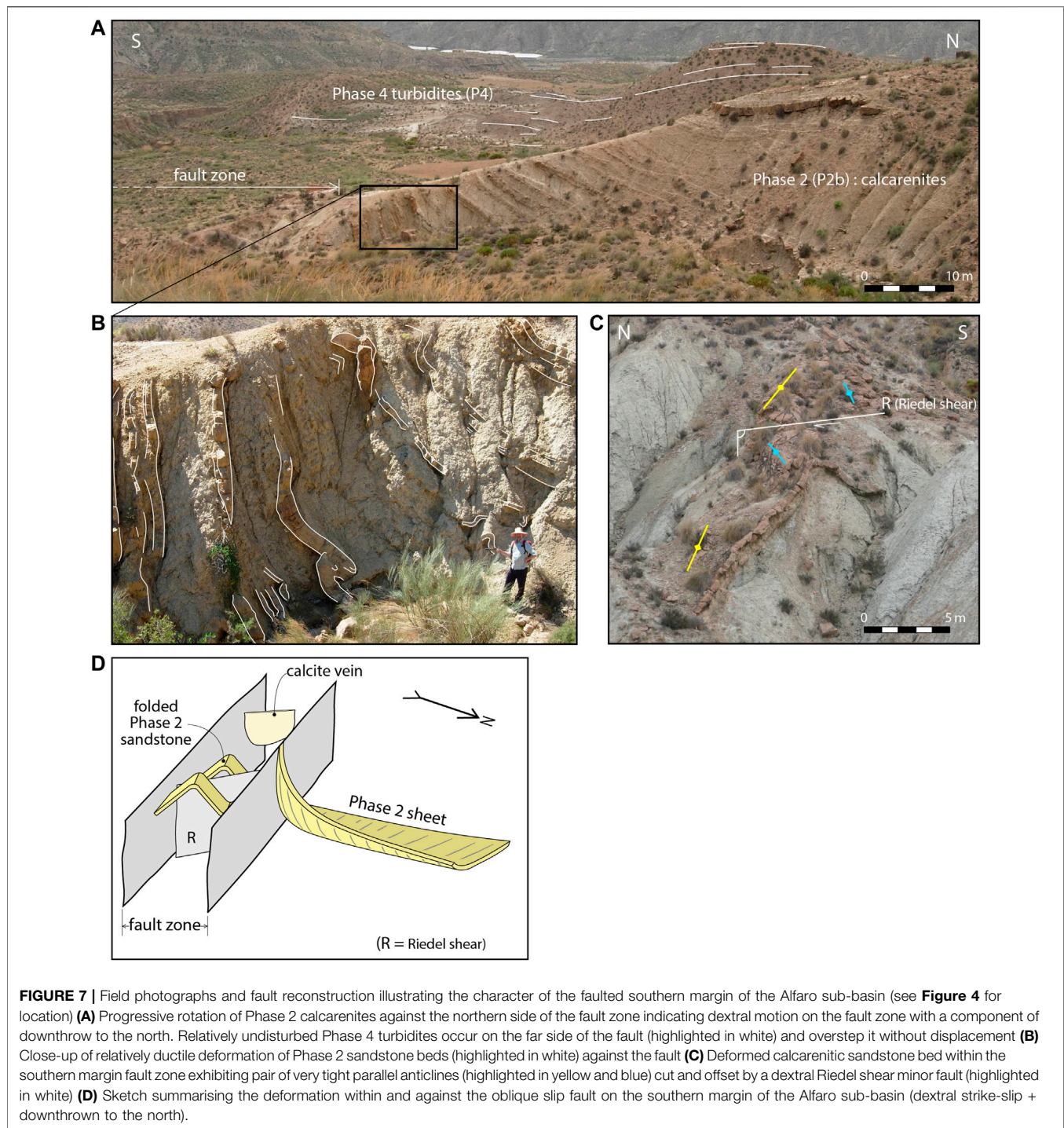
emplaced on mobile mud beds; turbidity currents may have either triggered local substrate flows or they may have interacted with mudflows released by the same external trigger (see below). The strongly layered nature of the sheet succession with sands encased in marls may have encouraged packet sliding off low gradient slopes, with gravity deformation continuing by brittle deformation and shallow faulting after emplacement of the sandstone and its associated mudstone cap.

4.3 Southern Margin of Sub-basin

The Alfaro Member calcarenites and overlying Phase 3 ponded turbidites can be followed southwards off the Alfaro ridge to the area north of Rambla de Indalecio where a series of exposures constrain the stratigraphic and structural geometry of the southern margin of the sub-basin. When traced down the dip slope to the southwest, the Alfaro Member calcarenites and basal part of the ponded sheets are overstepped by the Phase 4 basin fill. In the Barranco de los Baños, the Alfaro calcarenites are overlain by the basal part of the ponded sheet succession which is discordantly overlain by upper Phase 3 sheets. The result is that only a thin and incomplete interval (c. 50 m thick) of the Phase 3 fill is developed here (compared to >300 m to the north). Further south again, Alfaro calcarenites that floor the sub-basin to the north are progressively rotated to near vertical and juxtaposed against pale grey scaley marls by a decametre-wide vertical fault zone trending N090E (**Figure 7**). Ductile deformation of the adjacent, now cemented and brittle, calcarenites suggest that they were cohesive but not fully lithified at the time of deformation (**Figure 7B**). Mode I vuggy calcite veins occur in the fault zone and these have an average strike of N155E. Some sub-vertical dextral E-W shear planes are also developed in this fault zone and are occasionally

utilised by fibrous calcite veins. When the fault is traced 400 m to the east, calcarenites flanking the fault are incorporated into the fault zone and deformed to produced folds with axes orientated N070E which were then cut by minor N120E-trending dextral faults (**Figure 7C**). To the south of the fault, Alfaro calcarenites are not present, and Phase 2 marls are directly overlain by Phase 4 sheet turbidites. The contact is a sharp surface, generally planar but with local steps, against which the younger succession systematically onlaps in a south-easterly direction. The onlapping succession also contains evidence for significant gravity-induced deformation directed away from the slope (discussed in more detail below). The mapped distribution of the Phase 4 turbidites implies they extend without displacement across the shaley gouge zone that truncates the Alfaro calcarenites.

Interpretation: The scaley and calcite-veined gouge resembles a thinner version of the anomalously thick gouge zone bounding the northern side of the sub-basin. It is similarly interpreted as a syn-depositional fault, the key evidence being the overstep of the younger Phase 4 stratigraphy and the Gordo megabed embedded in it across the fault trace without displacement. The southern fault zone is orientated ENE-WSW and projects eastwards into a dextral step in the basement of c. 1 km. Overall the two bounding faults are slightly oblique to one another in map view and they converge to the east. As late uplift and subsequent erosion have produced an oblique slice, the geometry is interpreted as upward splaying of the principal displacement zone with the sub-basin sitting between two active strands of the same linked fault system. Small scale internal deformation features and vein orientations indicate the fault bounding the sub-basin to the south was a dextral fault zone (like the El Cautivo Fault

FIGURE 7 | Field photographs and fault reconstruction illustrating the character of the faulted southern margin of the Alfaro sub-basin (see **Figure 4** for location) **(A)** Progressive rotation of Phase 2 calcarenites against the northern side of the fault zone indicating dextral motion on the fault zone with a component of downthrow to the north. Relatively undisturbed Phase 4 turbidites occur on the far side of the fault (highlighted in white) and overstep it without displacement **(B)** Close-up of relatively ductile deformation of Phase 2 sandstone beds (highlighted in white) against the fault **(C)** Deformed calcarenitic sandstone bed within the southern margin fault zone exhibiting pair of very tight parallel anticlines (highlighted in yellow and blue) cut and offset by a dextral Riedel shear minor fault (highlighted in white) **(D)** Sketch summarising the deformation within and against the oblique slip fault on the southern margin of the Alfaro sub-basin (dextral strike-slip + downthrown to the north).

Zone) but in this case with a component of downthrow to the north (**Figure 7D**). Deformation flanking the fault zone to the south and/or longer wavelength uplift linked to the rise of the basement blocks may have tilted the muddy Phase 2 succession down to the north to provide the relatively smooth slope against which the younger Phase 4 stratigraphy laps out. The change from Phase 3 to Phase 4 turbidites coincides with overfilling of the sub-basin and a switch to deposition

over a wider area that draped the then-inactive faults and onlapped an unstable confining slope to the south.

4.4 Sub-Basin Fill and Stratigraphic Geometry

The sub-basin lying between the two fault strands is c.2 km wide and dominated by a succession of laterally extensive Phase 3
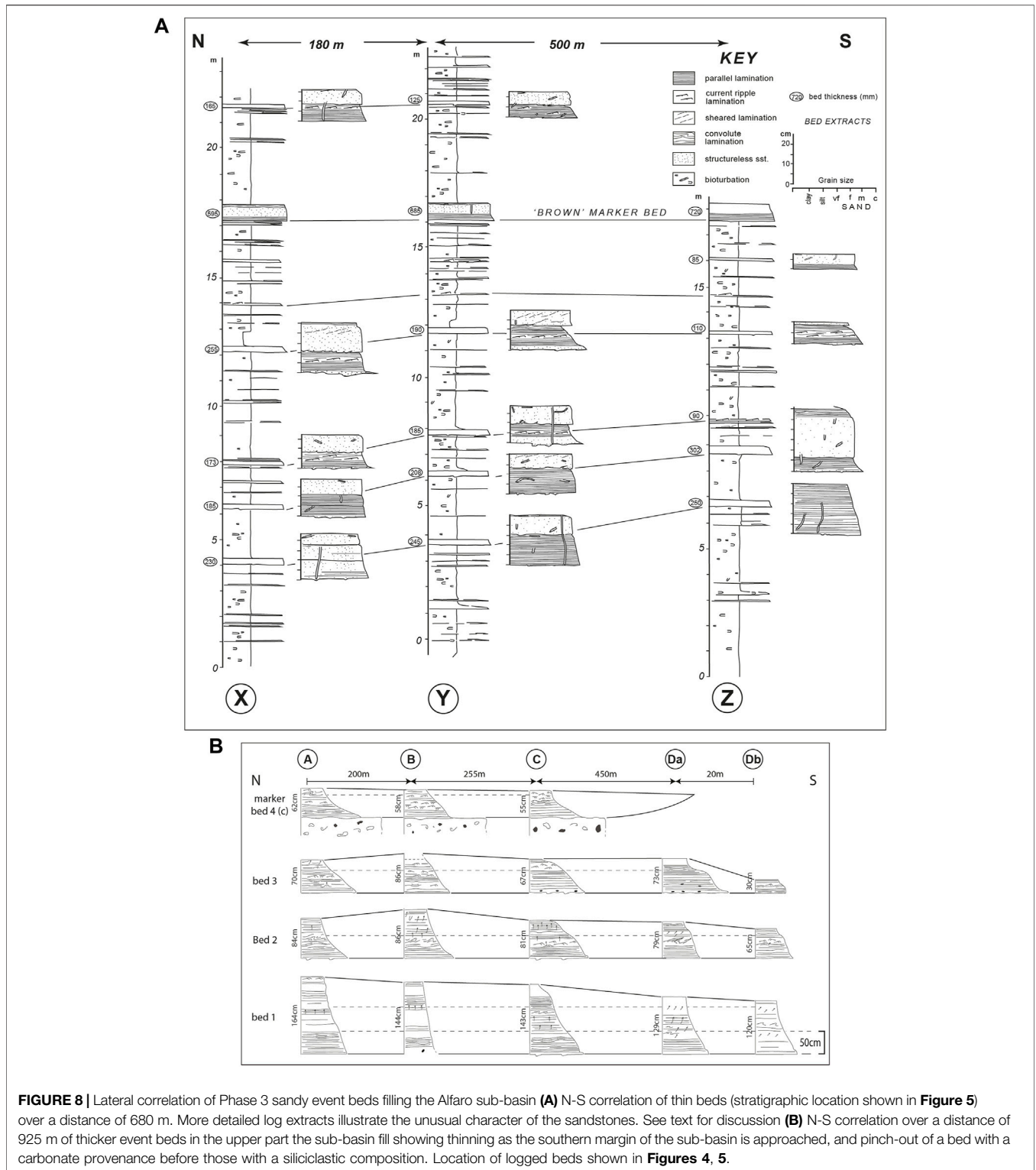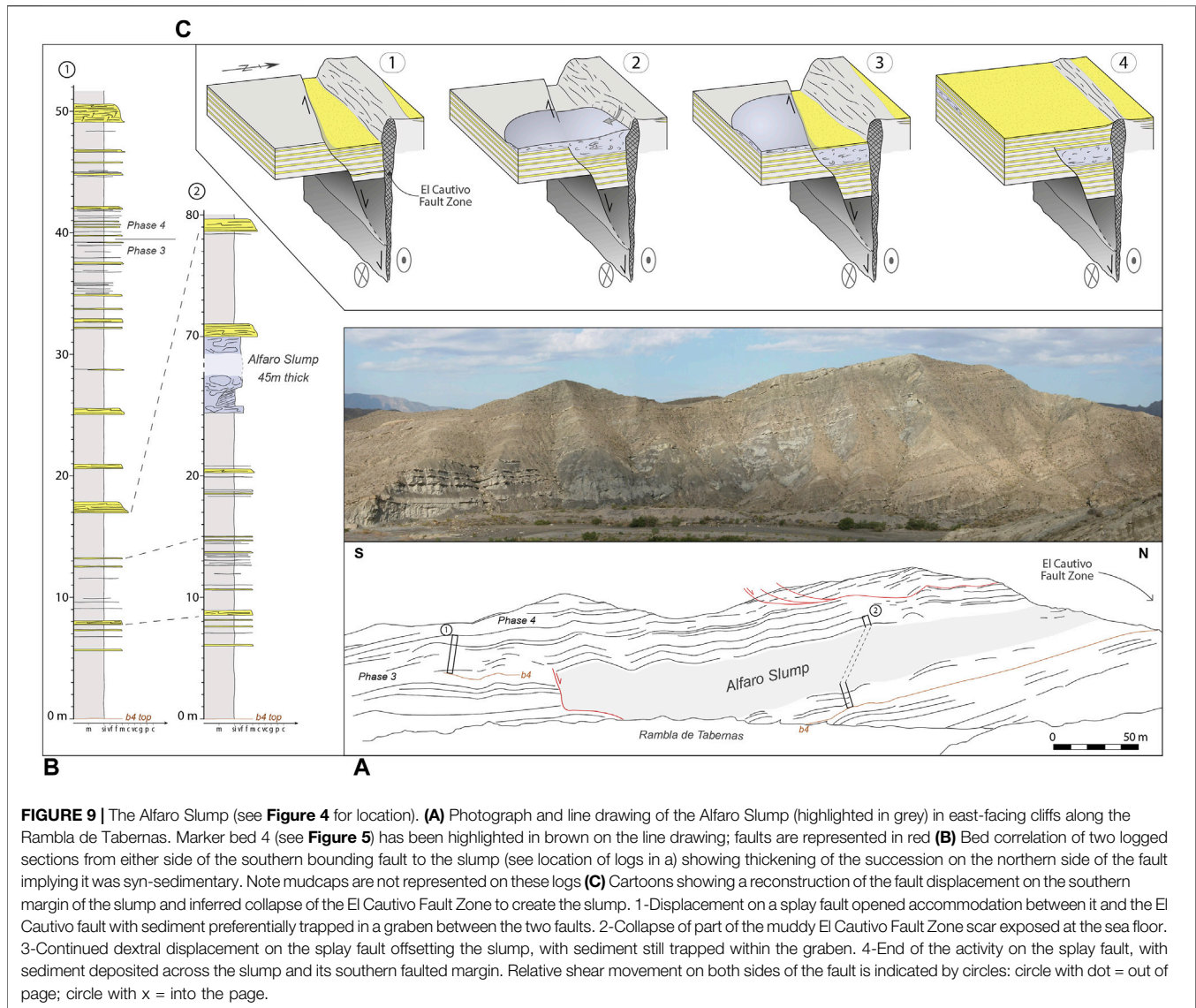
FIGURE 8 | Lateral correlation of Phase 3 sandy event beds filling the Alfaro sub-basin **(A)** N-S correlation of thin beds (stratigraphic location shown in **Figure 5**) over a distance of 680 m. More detailed log extracts illustrate the unusual character of the sandstones. See text for discussion **(B)** N-S correlation over a distance of 925 m of thicker event beds in the upper part the sub-basin fill showing thinning as the southern margin of the sub-basin is approached, and pinch-out of a bed with a carbonate provenance before those with a siliciclastic composition. Location of logged beds shown in **Figures 4**, **5**.

ponded turbidite sheets (Haughton, 2000; Hodgson and Haughton, 2004) up to 300 m thick (**Figure 5**). The younger of these sheets extend across the full width of the sub-basin. They are dominantly siliciclastic sandstones, but include at least 5 sheets with a carbonate provenance (in all cases debrite-turbidite

couplets with the sand fraction dominated by bioclastic grains). A distinctive bundle of closely spaced beds c.140 m below the top of the sub-basin fill (highlighted on **Figure 5**) can be traced laterally between sections. Three stacked siliciclastic turbidite sheets (referred to as beds 1, 2 and 3) and an overlying calcarenite

FIGURE 9 | The Alfaro Slump (see **Figure 4** for location). **(A)** Photograph and line drawing of the Alfaro Slump (highlighted in grey) in east-facing cliffs along the Rambla de Tabernas. Marker bed 4 (see **Figure 5**) has been highlighted in brown on the line drawing; faults are represented in red **(B)** Bed correlation of two logged sections from either side of the southern bounding fault to the slump (see location of logs in a) showing thickening of the succession on the northern side of the fault implying it was syn-sedimentary. Note mudcaps are not represented on these logs **(C)** Cartoons showing a reconstruction of the fault displacement on the southern margin of the slump and inferred collapse of the El Cautivo Fault Zone to create the slump. 1-Displacement on a splay fault opened accommodation between it and the El Cautivo fault with sediment preferentially trapped in a graben between the two faults. 2-Collapse of part of the muddy El Cautivo Fault Zone scar exposed at the sea floor. 3-Continued dextral displacement on the splay fault offsetting the slump, with sediment still trapped within the graben. 4-End of the activity on the splay fault, with sediment deposited across the slump and its southern faulted margin. Relative shear movement on both sides of the fault is indicated by circles: circle with dot = out of page; circle with x = into the page.

sheet (marker bed 4) have a relatively constant thickness when traced north to south across the sub-basin floor for 800 m (**Figure 8B**), but thin as they approach the fault corridor at the south side of the sub-basin where the calcarentic sheet pinches out completely, implying it thins laterally at a faster rate than siliciclastic sheets of similar thickness. Complete pinch out of the siliciclastic sheets cannot be demonstrated due to lack of outcrop in the main rambla bed. N-S section correlations of relatively thin sheets at a deeper stratigraphic level demonstrate subtle but systematic southward thinning of the succession, mainly involving thinning of the bioturbated sandy marls between the sheet sandstones (**Figure 8A**). Beneath the sheet succession, a marl interval occurs in the central sub-basin, resting on top of the Alfaro Member calcarenites. This marl is absent to the south where sheet sandstones higher in the section directly overlie the Alfaro Member. Just north of the Barranco de los Baños large calcarenite sandstone blocks (up to 70 m across) occur locally interleaved with the Phase 3 stratigraphy.

A major remobilised unit (referred to here as the Alfaro Slump; **Figure 9**) is intercalated with sheet turbidites within the sub-basin fill (c. 75 m below the top of Phase 3), but only in the northern part of the sub-basin. This is well exposed in high cliffs on the western margin of the Rambla de Tabernas (**Figure 9A**) immediately south of the El Cautivo Fault Zone. The slump is 45 m thick and is composed of chaotic sheared muddy matrix (more than 90%) with scattered deformed sandstone blocks (up to 1 m across) as well as poorly defined marl blocks which are recognised by their bedding-discordant fissility. It has a sheet-like geometry with no convergence of turbidite beds above and below. The slump has a planar base with the underlying marls and it sits stratigraphically above a distinctive calcarenite debrite-turbidite couplet (marker bed 4; see above). When followed to the north, the slump can be traced to within 10 s m of the El Cautivo Fault although recent erosion means the actual contact is no longer preserved. Sheet turbidites beneath the slump extend to and are truncated by the fault zone

and a similar relationship is inferred for the slump unit. No correlative of the slump can be found in the Phase 3 succession north of the El Cautivo Fault Zone. The slump can be followed 300 m south, along the Rambla de Tabernas to a sharp bend in the river where another fault with a strike of N120E truncates both the slump and underlying turbidite beds. The fault plane is sharp with a stepped geometry; a sub-vertical segment truncates the upper part of the slump, but the fault flattens close to ramble level. Significantly, the slump cannot be identified in the exposures south of the fault (contrast with Hodgson and Haughton, 2004). The geometry and timing of fault displacements have been documented by carefully logging the succession straddling the fault (**Figure 9B**) and by tracing beds using detailed photomontages. Marker bed 4 is displaced vertically c. 60 m by the fault. On the downthrown side (to the north), there are two bundles of thin beds in the 25 m thick section below the slump. Only the lower of these can be identified south of the fault in a similar position relative to bed 4. The slump cannot be correlated across the fault, but the turbidites above it forming the upper half of the cliff do not appear to be affected by the fault. Indeed the bed located at 17 m on the log south of the fault oversteps the fault and corresponds to the second thick bed above the slump (at 79 m on the northern log). The topmost beds on the cliff are composed of the lowermost beds of the Phase 4 (post sub-basin) fill. The boundary is placed at a step increase in the frequency of thin beds.

There is no bedding discordance at the top of sub-basin fill in the northern part of the sub-basin. However, the transition from Phase 3 isolated ponded sandstone sheets to Phase 4 fill is reworked by a major mass transport deposit in the southern part of the sub-basin (MTD-1 described in detail below). When the sub-basin fill dips are flattened by restoring the mean Phase 4 fill dips to horizontal, the residual dip is to the north implying tilting towards the El Cautivo Fault.

Interpretation: Filling of the sub-basin took place mainly by suspension settling of muds interspersed with sporadic turbidity currents, the larger volume of which became ponded and evolved to higher concentrations as sustained flows continued to drain into what must have been a relatively small bathymetric deep. Although the margins of the sub-basin are faulted, it was probably not greatly wider than the 2 km currently preserved. The strike extent of the sub-basin is speculative as it dips beneath younger stratigraphy to the west, and its eastern extent has been removed by erosion. Evidence for a thicker succession in the northern part of the sub-basin, thinning of individual sheets as the southern margin is approached, residual dip to the north and local angular discordances in the south suggest a wedge-shaped profile with greatest subsidence in the north. Tectonically-induced facies asymmetry has been noted in other deep-water basins, notably the Peïra Cava Basin, SE France (Cunha et al., 2017) and the northern Apeninnes, Italy (Tinterri et al., 2017). If the Alfaro Member calcarenites fill channels at the base of the sub-basin as is suspected, their distribution (thicker to the south and lapping out to the north) implies initial subsidence may have been focussed further south and then migrated to adjacent to the main fault strand in the north when this propagated to the sea floor. Blocks of calcarenite within the sheet turbidites close to the

southern margin imply tilting may have led to uplift and reworking of the Alfaro Member next to the southern boundary fault.
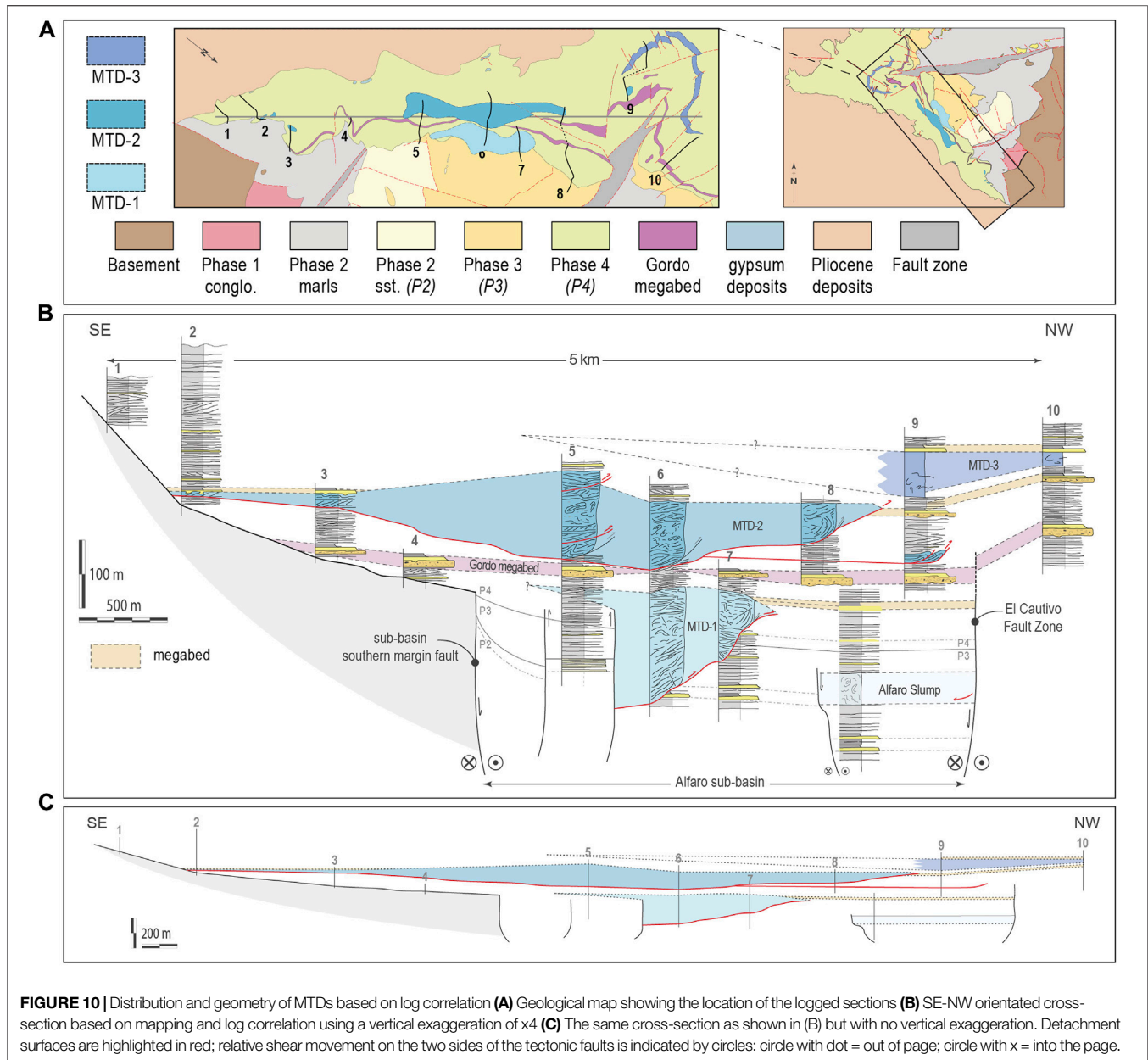
Younger Phase 3 sheets (and the marls between them) vary little in thickness across the floor of the sub-basin implying this was sub-horizontal by this stage. Thinning adjacent to the southern margin of the sub-basin reveals the presence of a fault-controlled, bounding slope. More rapid pinching out of the calcarenitic compared to the siliciclastic flows suggests a difference in the flow characteristics. The former may have been thinner with more concentrated lower portions as they tend to be coarser grained with less silty and micaeous components. The ponded suspensions may have inflated to differing extents, explaining the difference in pinchout geometry.

The thick interbedded slump has been attributed to local collapse of part of the El Cautivo Fault scar (Haughton, 2000; Hodgson, 2002). This is consistent with the muddy composition of the slump and its position adjacent to the El Cautivo Fault Zone. The analysis of the intra sub-basin fault limiting the slump to the south demonstrates that it was also active during deposition, initiating after the first bundle of thin beds above the bed 4 marker and ending shortly after slump deposition. The fault temporally partitioned the floor of the sub-basin providing deeper accommodation between it and the El Cautivo Fault. Occasional turbidity currents arriving from the west were preferentially trapped and confined on the downthrown block between the two faults (**Figure 9C**). Superficially the fault to the south appears extensional, but this would require an unrealistically high (>50 m) scarp to totally confine the slump. The major cross-sectional bend (step) on this fault requires a strike-slip component of displacement; furthermore bed geometries of sequences adjacent to this curved fault are incompatible with significant dip-slip displacement (**Figure 9A**). The preferred interpretation is therefore that the fault has laterally displaced the slump so that any overstep of the fault by the slump is out of the plane of section (**Figure 9C**); i.e. now below the ground for a dextral offset. The proximity and the angle between the faults bounding the slump suggest the small fault to the south formed a synthetic fault splaying from the dextral El Cautivo Fault.

The conformable contact between the Phase 3 sub-basin fill and the overstepping Phase 4 succession implies the fault-induced wedging and lateral displacement of the sub-basin had finished before Phase 4 deposition when the linked faults became inactive.

5 POST-FILL SLOPE ONLAP AND MASS WASTING

The overstepping Phase 4 succession progressively onlaps and wedges out against a rotated Phase 2 muddy succession directly south of the sub-basin. The Phase 4 turbidites show common evidence for sliding with rotated and internally-deformed bed packages several 10 s of m thick (e.g. in the Rambla de Indalecio). In addition, there are also three large mass transport deposits (MTDs 1–3) that rework the onlap wedge and slope. The MTDs

FIGURE 10 | Distribution and geometry of MTDs based on log correlation **(A)** Geological map showing the location of the logged sections **(B)** SE-NW orientated cross-section based on mapping and log correlation using a vertical exaggeration of x4 **(C)** The same cross-section as shown in (B) but with no vertical exaggeration. Detachment surfaces are highlighted in red; relative shear movement on the two sides of the tectonic faults is indicated by circles: circle with dot = out of page; circle with x = into the page.

partly drape (and in the case of the oldest one, rework) the former fault-controlled sub-basin and they are enclosed largely within Phase 4 sheet turbidites. The larger scale architecture of the onlap-wedge has been captured in a series of logs (**Figure 10**) along a 5 km long SE-NW orientated transect that is approximately parallel to the slump transport direction. The three MTDs form lensoid bodies the thickest parts of which step basinwards with time. In addition, a very thick debrite-turbite couplet (the Gordo Megabed) occurs between MTD-1 and -2 and onlaps directly onto the north-facing slope.

5.1 MTD-1

MTD-1 differs from the younger failures in that it remobilised both Phase 4 and Phase 3 deposits. It is very well exposed in the

Rambla de Tabernas and in nearby road cuts giving a particularly good 3D insight into its internal structure and relationship to the undisplaced stratigraphy (**Figure 11A**). MTD-1 is up to 160 m thick centrally and about 50 m thick close to its toe. It can be followed laterally for up to 600 m, and extends about 350 m across the top of the sub-basin which it partly reworks. Phase 3 and 4 turbidite beds incorporated in MTD-1 are largely intact albeit complexly deformed, so much of the remobilisation can be classified as a slump (sensu Martinsen, 1994). In low cliffs on the east side of the Rambla de Tabernas, the basal detachment to the MTD is seen. This is a planar, bedding parallel bundle of clay-lined surfaces that lies stratigraphically about 10 m above marker bed 4 in the Phase 3 sub-basin fill (see earlier). The surfaces separate lensoid bodies of imbricated sandstone beds (duplexes)
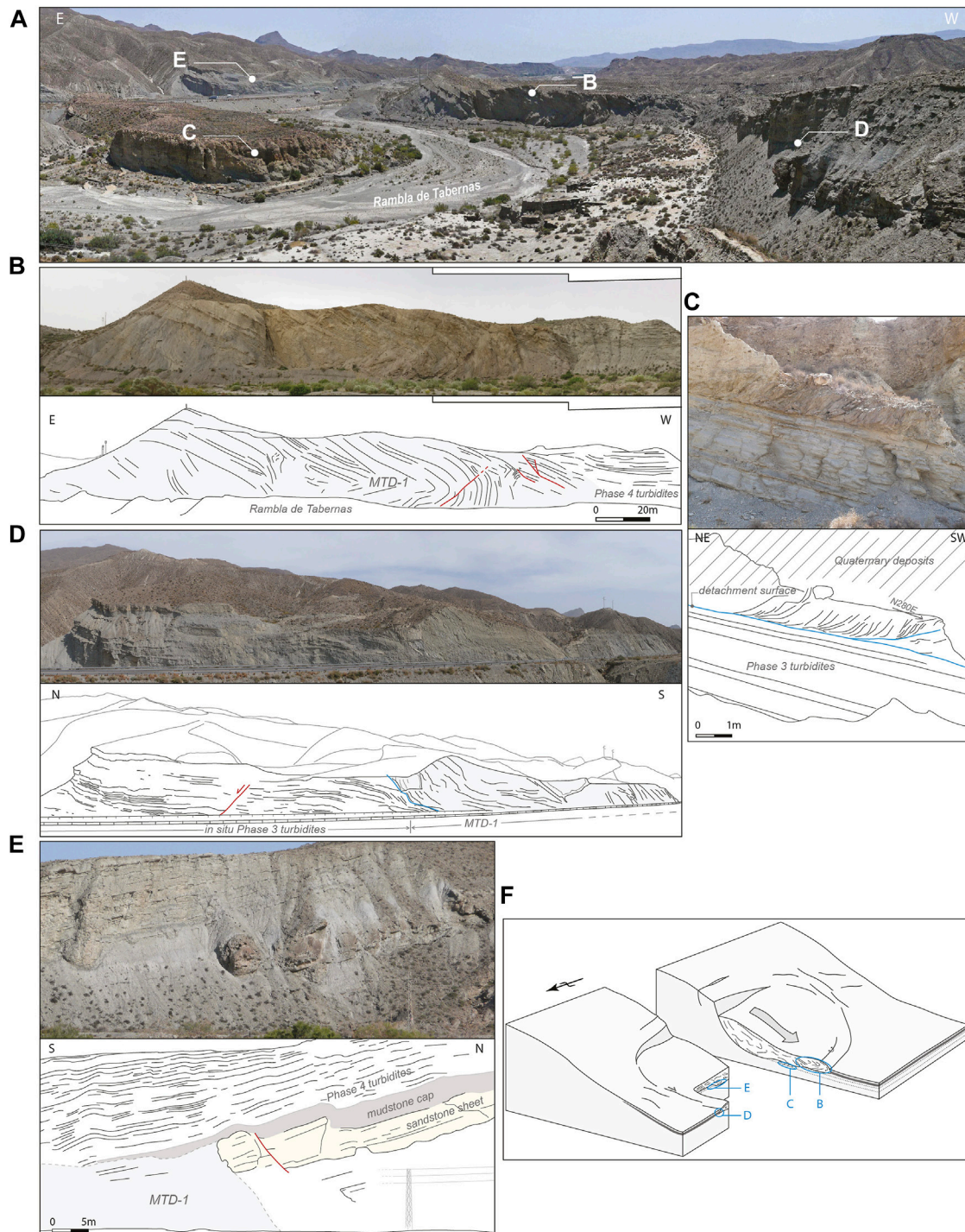
FIGURE 11 | Character of MTD-1 (see **Figure 4** for location) **(A)** General panorama of MTD-1 outcrops looking south down Rambla de Tabernas **(B)** Photograph and line drawing of a large recumbent fold at the toe of MTD-1 (highlighted in grey). In-situ Phase 4 turbidites draping the toe of MTD-1 occur on the western side of the outcrop. Faults developing within the fold are highlighted in red **(C)** Photograph and line drawing of the basal detachment zone characterised by the presence of duplexes formed by deformation of Phase 3 turbidites above the detachment surface (highlighted in blue). A westwards transport direction is deduced from the duplex orientation **(D)** Photograph and line drawing of the lateral detachment (blue) of MTD-1 (in grey) cutting through Phase 3 turbidites here observed along the N340 road **(E)** Photograph and line drawing of a Phase 4 megabed truncated by MTD-1 (highlighted in grey). Note the geometric relationship between the MTD and the megabed with the sandstone division of the megabed (highlighted in yellow) cut vertically by the lateral edge of the MTD but with the mudstone cap (highlighted in dark grey) overstepping the MTD **(F)** Schematic block diagram illustrating the 3D structure of MTD-1 (modified from Bradley and Hanson (1998)). The letters refer to the different components of the MTD illustrated in the preceding parts of the figure.

ranging from a few centimetres to a few tens of centimetres high. The slump transport direction deduced from the bed imbrication is from east (N100E) to west (**Figure 11C**).

The toe of MTD-1 is seen in a north-facing cliff (20 m high and 100 m long) at a prominent bend in the Rambla de Tabernas (**Figure 11B**). The basal detachment here is at rambla level and it has ramped up to within the overstepping Phase 4 turbidites. The ramp between here and where the basal detachment occurs on the east side of the rambla is estimated to be 40 m high. Both Phase 3 and 4 sheet turbidites are rafted intact above the detachment but roll into a large recumbent fold that is inclined to the west and corresponds to the toe of the failure. The toe is draped by in-situ Phase 4 turbidites in which there are many small dip discordances (**Figure 11B**).

Approximately 200 m to the north, MTD-1 truncates a 5 m thick sandstone sheet which can be mapped northwards away from the slump as part of an undisturbed succession of Phase 4 sheet turbidites. The thick sandstone is cut vertically by the lateral (northern) edge of the MTD, but a thick mudstone cap overlying the sandstone appears to overstep the junction between sandstone and the remobilised deposits, thinning and lensing out southwards over the MTD (**Figure 11E**).

MTD-1 is also seen beside the old N340 road in a high and unstable cut face north of Barranco de los Baños (a 300 m long and 30 m high exposure; **Figure 11D**). The northern end of the cliff preserves Phase 3 turbidite sheets (c. 50 m below marker bed 4), these are flexed down into MTD-1 which dominates the southern end of the exposure. Soft sediment deformation here has thus cut deeper still into the sub-basin fill. The eastern extension and headwall of the failure cannot be observed as this part of the MTD has been removed by recent erosion.

Interpretation: Exceptional exposure conditions encountered in the Tabernas Basin permits the reconstruction of the 3D geometry of MTD-1 (**Figure 11F**). An important feature of MTD-1 is that it is composed of local basin floor deposits, including translated ponded turbidites with thick mud caps that can only have formed on a relatively flat and deep part of the palaeo-sea floor. Phase 3 sandstone sheets preserved beneath the failure show evidence for thinning to the south suggesting proximity to a slope. Phase 4 turbidites that overstep the faulted southern margin of the sub-basin are also involved in the failure. A possible explanation is that gravity instability took place by sliding of the initial onlap wedge off the slope flanking the south-side of the sub-basin. This slide then interacted with and drove deformation of the earlier sub-basin fill. However, kinematic evidence from the stepped basal detachment, forced folds within the sliding mass and the position of the lateral limit of the failure suggests dominantly westward transport, parallel to the sub-basin margin. This suggests that failure may have been influenced by down to the west rotation of the sub-basin and its flanking slope (the Sierra Alhamilla to the east was uplifted to became emergent around this time). The large frontal fold may relate to a ramp on the underlying detachment, and to buttressing at the toe of the MTD. Minimal internal disaggregation is seen, at least in the section provided by the outcrop, consistent with limited transport and a low drop height due to the early stage in the onlap; MTD-1 involved slumping and sliding, but no transformation to a debris flow.

The trigger for the failure is uncertain, but the relationship with a large sandstone-mudstone couplet in the laterally equivalent undisturbed section to the north may be significant. The slump appears to cut the sandstone component of this bed, but to be onlapped by the mud produced by suspension fallout. This suggests MTD-1 may have been contemporary with a large-volume turbidity current, with failure occurring after the sand had fallen from suspension, but before the mud cloud rained out. Such a relationship could reflect a common trigger (seismic shaking) or a role for the large-volume (sloshing?) turbidity current in destabilising or loading the slope it impinged on. The former (common trigger) is perhaps less likely as the local slope failure might be expected to precede the arrival of the turbidity current.
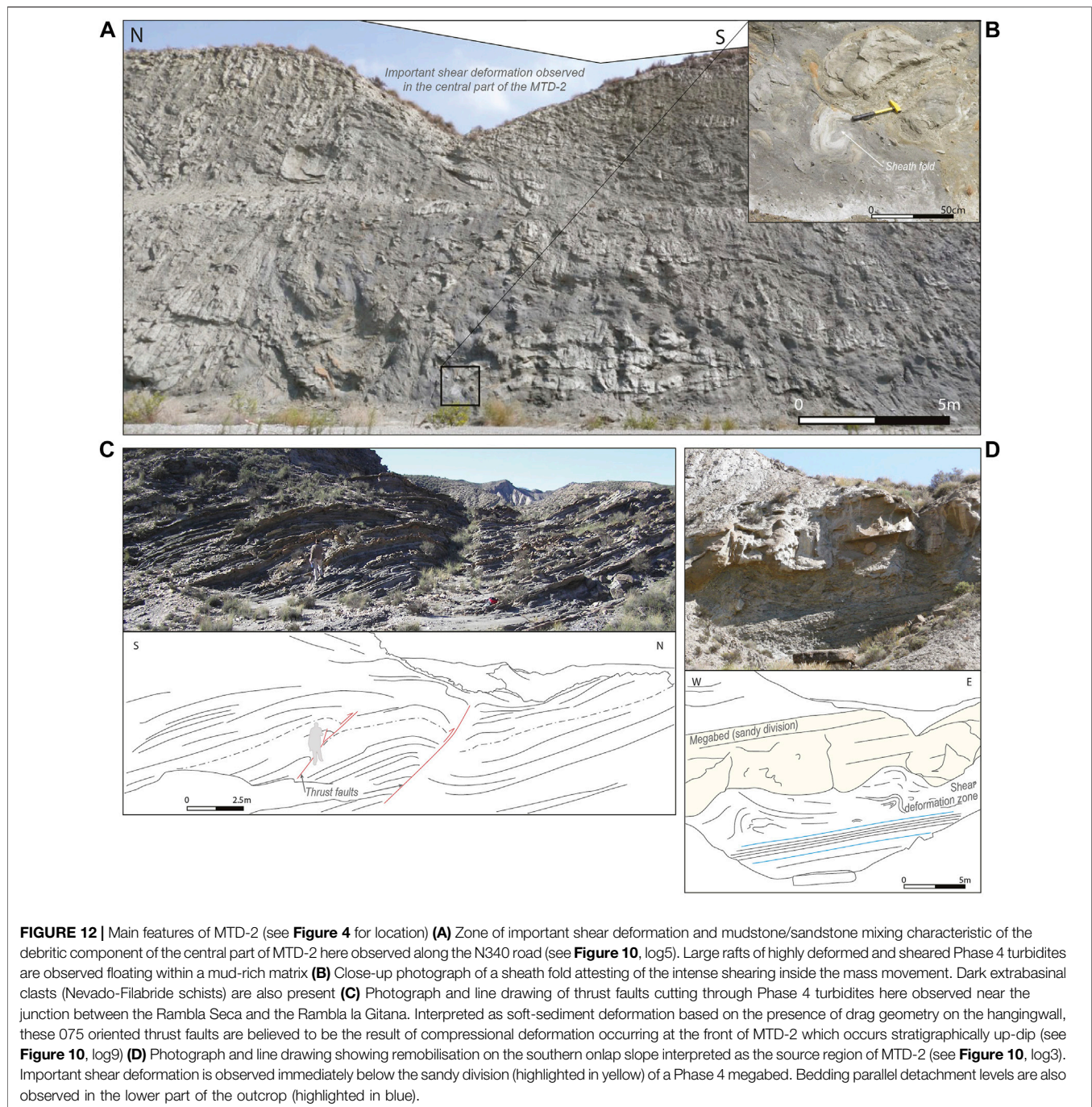
5.2 MTD-2

A second more extensive slope failure associated with the southern onlap slope occurs approximately 20–80 m above the Gordo megabed although locally it cuts down to the level of the Gordo megabed. MTD-2 can be traced between a series of outcrops for a distance of c. 3.5 km parallel to the SE to NW transport direction (**Figure 10**) using the underlying Gordo event bed as a marker. Its width is unclear due to outcrop limitations. MTD-2 blanketed the southern part of the underlying sub-basin, and was sourced higher on the southern onlap surface. It is up to 130 m thick and characterised by a variable degree of internal disaggregation, locally forming blocks dispersed in a well-mixed matrix. The style of deformation also varies laterally along the failure. MTD-2 translated Phase 4 basin floor turbidites downslope, with no evidence for input of external slope-derived sediment. It does, however, locally contain pebbles and cobbles of Nevado-Filabride schist.

Close to the onlap surface (approximately 200 m from the projected onlap, and 100 m above the Gordo event bed), the inferred head region of the failure is seen. Here, a 6 m thick package of discordant inclined beds is overlain by a sandstone/ mudstone couplet with an irregular base. When traced c.100 m to the NW, the basal deformed zone becomes more complex with several internal detachment levels (**Figure 12D**). There is also an increase in the deformation intensity with local folding beneath an irregular contact with the overlying sandstone-mudstone couplet.

A farther 1.8 km downslope, a large fresh road cut through the failure (200 m long and 15 m high) just south of Barranco de los Baños shows the deformation cuts down to within 20 m of the Gordo megabed (**Figure 12A**). The MTD here comprises upper and lower packages of soft-sediment deformed but coherent turbidites sandwiching a highly sheared and remoulded central part. The latter includes sheath folds (with SE-NW orientated stretching) and large (6 m across) folded and locally overturned rafts of Phase 4 turbidites floating in a poorly sorted, mud-rich matrix (**Figures 12A,B**). Significantly, extrabasinal clasts (mainly black schist and quartz vein pebbles up to 10 cm across) also float within the matrix. Overall, the deformed zone is estimated to be 130 m thick.

MTD-2 is also seen on the west side of the Rambla de Tabernas in an east-facing cliff up to 20 m high and 250 m long. The upper part of the MTC has been removed by recent

FIGURE 12 | Main features of MTD-2 (see **Figure 4** for location) **(A)** Zone of important shear deformation and mudstone/sandstone mixing characteristic of the debritic component of the central part of MTD-2 here observed along the N340 road (see **Figure 10**, log5). Large rafts of highly deformed and sheared Phase 4 turbidites are observed floating within a mud-rich matrix **(B)** Close-up photograph of a sheath fold attesting of the intense shearing inside the mass movement. Dark extrabasinal clasts (Nevado-Filabride schists) are also present **(C)** Photograph and line drawing of thrust faults cutting through Phase 4 turbidites here observed near the junction between the Rambla Seca and the Rambla la Gitana. Interpreted as soft-sediment deformation based on the presence of drag geometry on the hangingwall, these 075 oriented thrust faults are believed to be the result of compressional deformation occurring at the front of MTD-2 which occurs stratigraphically up-dip (see **Figure 10**, log9) **(D)** Photograph and line drawing showing remobilisation on the southern onlap slope interpreted as the source region of MTD-2 (see **Figure 10**, log3). Important shear deformation is observed immediately below the sandy division (highlighted in yellow) of a Phase 4 megabed. Bedding parallel detachment levels are also observed in the lower part of the outcrop (highlighted in blue).

erosion at this site. The Gordo event bed is also missing in this outcrop and deformation associated with MTD-2 merges downwards with MTD-1 deformation, making the base of MTD-2 hard to pick. MTD-2 deformation at this site is characterised mainly by multiple slide surfaces and discordances, particularly low in the body, with an increase in strain towards the central part of the MTD where tight folds and complex internal disruption are observed in rafts floating within a homogenised matrix.

The toe of the failure can be reconstructed from outcrops in the area close to the junction of the Rambla Seca with the Rambla

la Gitana. Here a large overturned fold (at least 30 m wavelength) of Phase 4 turbidites is developed. Further to the NW, the post-Gordo succession is largely intact but traversed by several soft-sediment thrust and reverse faults and associated forced folds (**Figure 12C**). Restoration of the fault geometry indicates compression from the south-east.

Interpretation: MTD-2 differs from MTD-1 in that it preserves evidence for internal disaggregation and matrix formation. This suggests that this failure initiated as a slide but locally broke up internally to become a debris flow. Transformation of just the

central section of the MTD may reflect a combination of partitioning of deformation in the lower part to the basal shear surface and reduced drainage of water from the central part, increasing pore fluid pressure. Alternatively, the failure may have occurred in two phases. MTD-2 transported Phase 4 turbidites blocks and is interpreted to have formed by collapse of part of the onlap-wedge. The toe of the failure was associated with a large fold and it is interpreted to have been frontally-confined like MTD-1. Compressional deformation spread out down slope from the confined front, deforming the basin floor that buttressed the failure. Transport was to the NW on the basis of internal and external shear indicators and the geometry of the inferred frontal fold.

A thick debrite-turbidite or megabed occurs stratigraphically 80 m above the Gordo megabed in the southern Tabernas Basin away from the onlap slope. Extrabasinal pebbles incorporated in MTD-2 resemble those in northerly-derived, large-volume event beds and are unlikely to have come off the southern slope. The thick sandstone–mudstone couplet also blankets headwall slides and slumps close to the onlap. The association between slumping and sliding and the emplacement of a large megabed is again significant and may suggest a link.

5.3 MTD-3

The youngest failure, MTD-3, occurs approximately 110 m above the Gordo megabed and is more difficult to link to the onlap surface and turbidite wedge, partly because it crops out remote from the onlap to the south and west of the junction of the Rambla la Gitana with Rambla Seca, beyond the confined toe of the underlying MTD-2. Although it is displaced on a series of NE-SW trending faults, it can be mapped over a strike length of at least 1.5 km. It is up to 65 m thick and dominated by white marl in which are dispersed sparse deformed clasts and rafts (up 10 s m long) of distinctive pebble-bearing calcarenites (locally micro-conglomerates). The marl unit thins northwards to c. 15 m over 1 km. The rafts tend to be folded. Rounded pebbles as clasts and within the rafts are dominantly basement dolomite, the surfaces of which are extensively bored. The calcarenites contain extensive shell fragments, including corals. MTD-3 is directly overlain by a thick sandstone-mudstone couplet, so the overall appearance of the unit is of a debrite-turbidite couplet; however, the capping sandstone is not a calcarentite. It is a siliciclastic sand of metamorphic provenance similar to the bulk of the basin floor turbidites making up the Phase 4 basin fill.

Interpretation: MTD-3 was not derived from the onlap wedge, but from higher on the southern slope. The pebble types and calcarenitic composition of the rafts in the lower muddy unit suggest emplacement as a mudflow dispersed from a southern or southwestern source (possibly the Sierra de Gádor). Abundant borings and coral fragments suggest a partly shallow water source, not the deep water reworking of basin-floor turbidites seen in the older MTDs. Whereas MTDs 1 and 2 were slope-attached and frontally-confined, MTD-3 appears to have more passively filled deep bathymetry without disturbing the onlap wedge. It was directly followed by a contained turbidite, not a trailing plume from the mudflow but a separate event dispersed from a different (siliciclastic) source. The sharp switch in

composition implies that this is unlikely to a case of textural and compositional fractionation in a single flow. This again indicates a connection between different failure events, in this case possibly sharing the same trigger as there is little mixing between the two deposits. The stacking of event beds one on top of the other suggests little mounding on the top of the lower debrite, despite its thickness.

6 DISCUSSION

The re-analysis of the Tabernas Basin provides 1) new insight into the architecture of turbidite successions close to active faults and unstable slopes, and 2) improved understanding of the tectonic controls on sedimentation and Neogene basin development in this area of SE Spain.

6.1 Architecture of Turbidites Onlapping Active Slope Systems

Turbidity currents are commonly confined by lateral and/or distal slopes against which their deposits thin and pinch out. Outcrop examples of turbidites that can be traced laterally to onlap against slopes have been described from a number of basins (e.g. Sinclair 2000; McCaffrey and Kneller, 2001; Amy et al., 2004; Smith and Joseph 2004; Marini et al., 2015; Spychala et al., 2015). Most examples involve simple aggradation of confined turbidites against stable slopes that are either bare of sediment or draped by mud. Less is known about onlap settings where the onlap is inherently unstable and the slope/base of slope is modified by episodic slope failures, although this situation is likely to be common in basins on active substrates, such as slope mini-basins in the Gulf of Mexico and elsewhere (Madof et al., 2009; Beaubouef and Abreu, 2010) or thrust-top basins (Tinterri and Tagliaferri, 2015). Onlaps associated with the Alfaro sub-basin are instructive on a number counts:

Firstly, they show that the bed style can reflect the degree of confinement (see also Hodgson and Haughton 2004). Confined turbidites within the small sub-basin have a different vertical structure to those filling the enlarged but still confined basin once the sub-basin topography was healed. This is best seen in the thinner beds which in the Phase 3 fill comprise sandstone beds capped by structureless sandstone divisions interpreted as fallout from sandy suspensions ponded in local basin floor depressions. Once the depressions were filled, thinner turbidite beds show well laminated sandstone divisions throughout with evidence for flow reversals from ripple laminations. The flows reflected off the confining slopes but dissipated before sandy suspension clouds could form (a function of weaker containment).

Secondly, flows of different provenance (siliciclastic vs calcareous) can have different onlap geometries against the same slope. Calcarenitic sandstones pinch out laterally on the south side of the sub-basin before siliciclastic sandstones of similar thickness are lost. The former tend to be coarser grained and may have formed thinner flows and suspension clouds that did not inundate the slopes as much (McCaffrey and Kneller, 2001). The finer grained and polymodal siliciclastic flows produced thicker suspensions that extended further up slope.
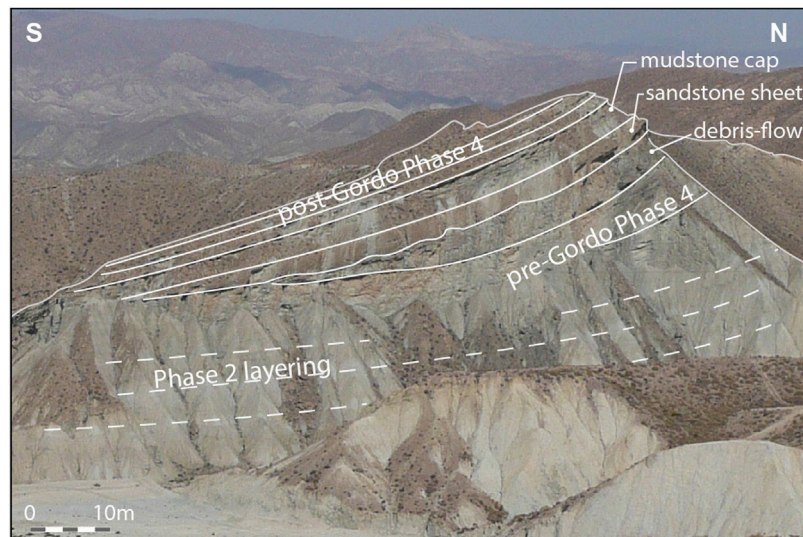
FIGURE 13 | Photograph and line drawing of the Gordo megabed onlapping directly onto tilted Phase 2 marls associated with the southern onlap slope (see **Figure 4** for location). Each division of the Gordo megabed (debris-flow, sandstone sheet and mudstone cap) pinches-out in turn against the slope.

Thirdly, when confinement is associated with an active fault, fault zone widening can trim the onlapping sandstones as has happened along the northern margin of the sub-basin. Ponded sheets show little thinning towards the fault due to the basin asymmetry, and are locally entrained as blocks in the fault zone.

Lastly, once the sub-basin was healed, the slope marking the southern limit of the basin was progressively onlapped but was subject to episodic collapse of the onlapping sediment wedge. Small scale slides involving thin bedded turbidites are common in the onlap area. Correlations using marker beds suggest a possible link between these slides and the thicker MTDs observed downslope on the floor of the basin. The slide complexes may record the instability leading to initiation of MTDs within the onlap wedge. MTDs 1 and 2 are composed mainly of wedge and basin floor turbidites and represent locally detached and frontally confined mass transport deposits with basal shear surface ramps, rafted blocks of remobilised turbidites, and well developed recumbent folds associated with frontal thrust propagation (Frey-Martínez et al., 2006; Moscardelli and Wood, 2008; Bull et al., 2009). The slump toes appear to have formed positive topography on the sea floor against which later turbidites onlap. MTD-3 was the furthest travelled and comprises exotic calcarenitic sandstone blocks, abundant borings, shells and coral fragments floating in a muddy background. The overall shape is also different with a more sheet-like geometry filling the deep bathymetry of the basin and draped by a thick ponded megabed (**Figure 10**).

Each of the local slope-sourced MTDs is associated with a thick, basin-wide megabed either lateral to it (MTD-1,-2) or directly on top of it (MTD-3). McCaffrey and Kneller (2001) drew attention to the possibility of debris flows triggered by turbidity currents impinging on distal slopes. Puigdefàbregas et al. (2004) describe outcrops of the Grés d'Annot onlap, SE France, showing evidence for deformation induced by flow

reflection against the basin confining slope. Overpressure in the slope muds associated with the sudden arrival of a large volume turbulent flow was thought to trigger injection, delamination and en-masse downslope movement. This sort of mechanism may explain the origin of MTD-1 and 2, particularly as large volume flows impinged on a slope that had been tectonically rotated and was being rapidly onlapped and loaded. One curious aspect of the slope stability is that the largest megabed event to impinge on the slope (Gordo megabed which occurred between MTD-1 and -2) did not trigger a failure. Instead, each of the three megabed elements (basal breccia or debrite, central graded sandstone and upper mudstone cap) lap out directly against the slope (**Figure 13**). It is possible the unusually thick basal debrite which contains abundant large intraclasts blanketed the slope protecting it from turbulent pressure fluctuations in the overlying expanded cloud. Alternatively, MTD-1 had already released the potential energy stored in the onlap wedge which was then relatively stable at this time.

This sort of distal failure triggering mechanism cannot apply for MTD-3 where the failure must have taken place high on the slope and did not involve remobilisation of the onlap wedge; the slope failure also preceded arrival of the megabed from a different source area. It is possible that in this case the separate slope failures had a similar trigger (a large earthquake?).

6.2 Tectonic Implications and Basin Development

Neogene basins in SE Spain have variously been interpreted as an extensional (Platt and Vissers, 1989; Vissers et al., 1995; Augier et al., 2005), thrust-top (Frizon De Lamotte et al., 1995) or strike-slip basins (Montenat et al., 1987a; Montenat et al., 1987b; Kleverlaan, 1989b; Haughton, 2000). The uncertainty
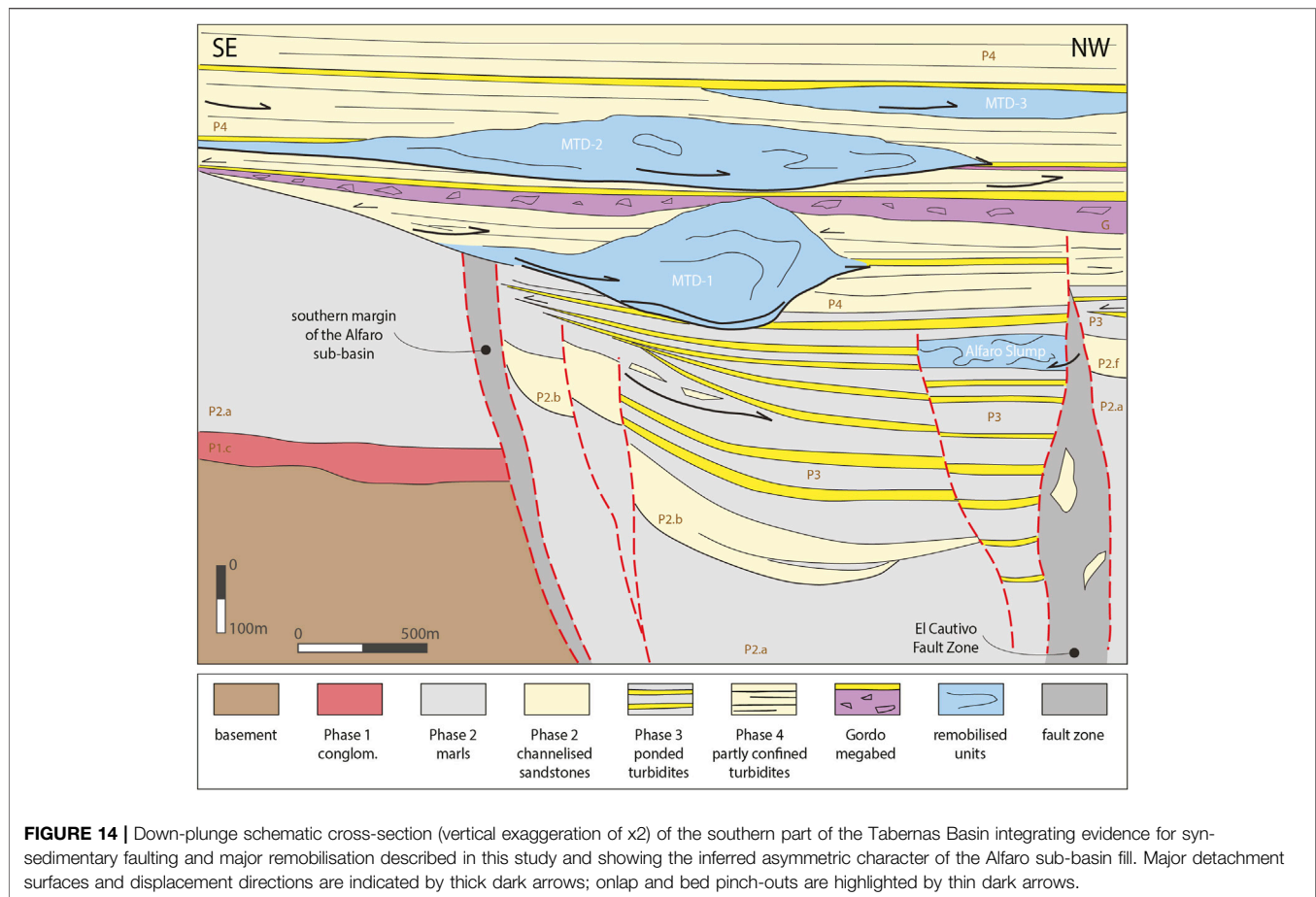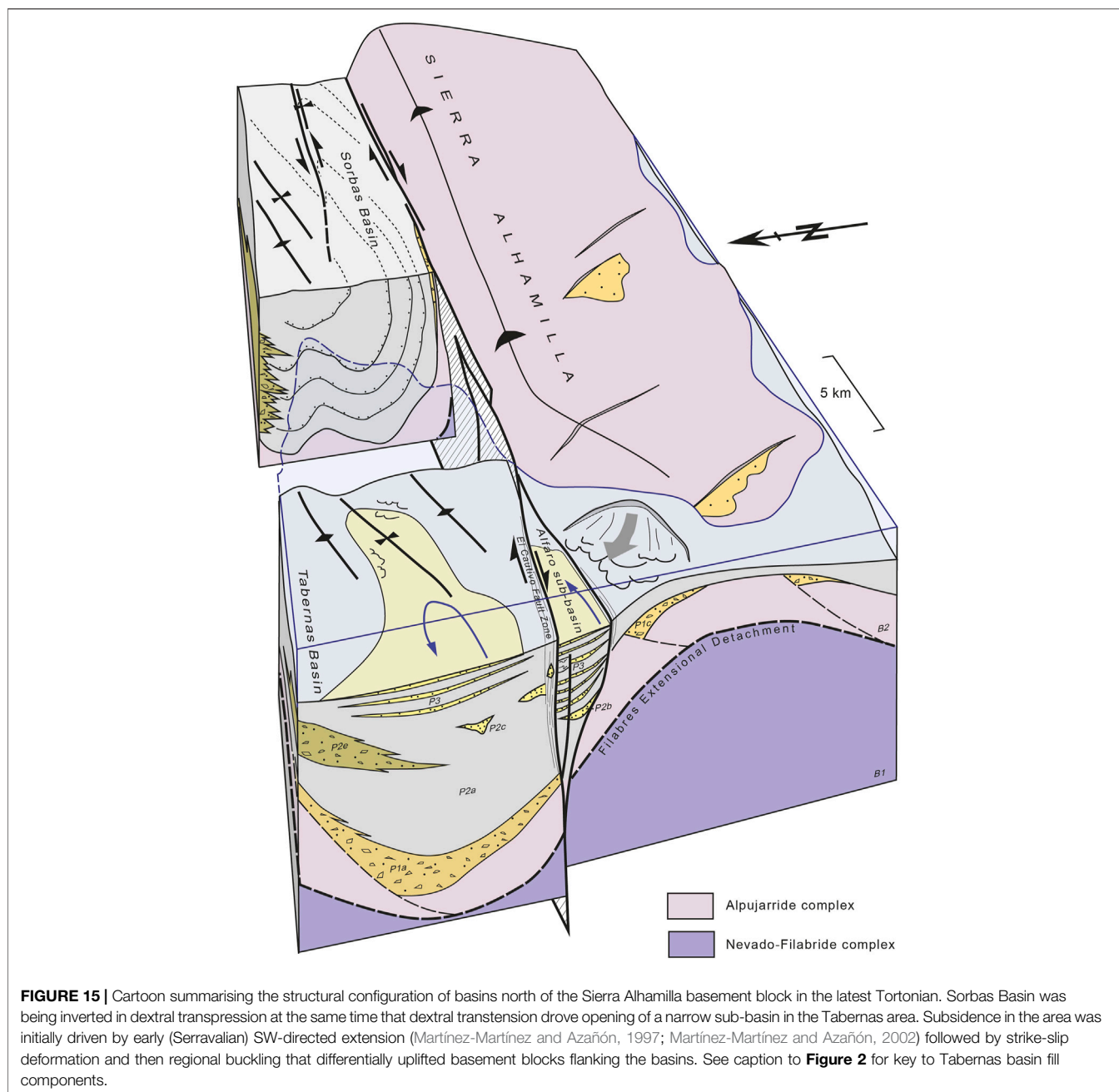
FIGURE 14 | Down-plunge schematic cross-section (vertical exaggeration of x2) of the southern part of the Tabernas Basin integrating evidence for syn-sedimentary faulting and major remobilisation described in this study and showing the inferred asymmetric character of the Alfaro sub-basin fill. Major detachment surfaces and displacement directions are indicated by thick dark arrows; onlap and bed pinch-outs are highlighted by thin dark arrows.

partly reflects the difficulty of linking faults to basin formation in areas where the stress field has evolved rapidly, where many of the faults are post-depositional, and where Neogene normal, thrust and strike-slip faults are all developed but are not necessarily directly related to basin formation. In addition, later rotation of earlier low-angle extensional structures to vertical can result in their misinterpretation as strike-slip faults (Valetti et al., 2019), and strike-faults can act as transfer structures in areas that are fundamentally undergoing heterogeneous extension (Martínez-Martínez, 2006; Giaconia et al., 2014).

Stratigraphic evidence discussed above (and in Hodgson and Haughton 2004) from the southern part of the Tabernas Basin strongly favours a strike-slip origin for the subsidence that opened up deep-water accommodation in that strike-slip faults are identified that were clearly active at the time of deposition. A wide range of different types of strike-slip basin have been described (e.g. Wood et al., 1994; Aksu et al., 2000; Lazar et al., 2006) ranging from fault-bend to stepover basins to basins formed between diverging or splaying faults. Other strike-slip basins form above relatively straight but divergent sectors of strike slip faults as negative flower structures (Bozkurt and Koçyiçğit, 1996; Aksu et al., 2000; Barnes et al., 2001) or due to transform-normal extension (Ben-Avraham and Zoback, 1992).

The Alfaro sub-basin formed a narrow trough delimited to north and south by oblique-slip faults that displaced the sea-floor. Subsidence was demonstrably asymmetric, thickening towards the fault with the more extensive gouge zone (the El Cautivo Fault) and with local unconformities and evidence for uplift and gravity sliding of earlier deposits along the southern margin (**Figure 14**). Splays of the main bounding fault also propagated through the fill, creating subtle irregularities on the sea floor, uplifting areas which modified the flow pathways and capturing a slump failure thought to relate to collapse of the master fault scarp. The syn-sedimentary oblique slip faults are interpreted to converge downwards and to link to a master fault. Outside and to the northeast of the sub-basin, a series of folds with fold axis trending at an angle of 30 anticlockwise to the E-W Alfaro fault zone also deformed the sea floor, creating depressions into which sheet turbidites thicken and highs that created local slope instability.

The convergence of dextral-oblique strike-slip faults at depth, evidence for displacements with important dip-slip components, the narrow trough-like sub-basin and the oblique orientation of folds suggest the sub-basin formed above a negative flower structure associated with a divergent strand of the fault that projects eastwards along the northern flank of the Sierra Alhamilla (Sanz De Galdeano, 1989; **Figure 15**). As bed dips in the vicinity of the Alfaro sub-basin are low, this cannot be an

FIGURE 15 | Cartoon summarising the structural configuration of basins north of the Sierra Alhamilla basement block in the latest Tortonian. Sorbas Basin was being inverted in dextral transpression at the same time that dextral transtension drove opening of a narrow sub-basin in the Tabernas area. Subsidence in the area was initially driven by early (Serravalian) SW-directed extension (Martínez-Martínez and Azañón, 1997; Martínez-Martínez and Azañón, 2002) followed by strike-slip deformation and then regional buckling that differentially uplifted basement blocks flanking the basins. See caption to **Figure 2** for key to Tabernas basin fill components.

example of earlier extensional detachments that have been rotated to vertical to masquerade as strike-slip faults as has been argued elsewhere (Valetti et al., 2019). Evidence for folding and ponding of turbidites north-east of the sub-basin imply lateral changes between coeval transtension and transpression. In the Rambla de Reinelo area, the sea floor was gently warped, but moving further east, the earlier fill to the Sorbas Basin was already inverted in strong dextral transpression at this time (Haughton, 2001). The eastward change to transpressional deformation corresponds with the position of the western culmination of the Sierra Alhamilla. Northward translation of the Alhamilla as the regional folds amplified in

the late Tortonian may account for this. The western end of the Alhamilla also marks a change in the style of turbidite deformation from strong ponding in deep depressions to the west, to weak ponding in shallow fold axes in the eastern Tabernas Basin. Hodgson (2002) also suggested that the Phase 2 sandy fan system exposed in the eastern part of the Tabernas Basin was deformed by growing transpressional folds during an earlier phase of bypass and basin floor fan growth. Close to Tabernas, early Phase 1 conglomerates were uplifted in the core of transpressional anticlines (**Figure 2**) against which the sandy fan onlapped. In the Sorbas area close to Lucainena (c.25 km to the east; **Figure 1**) Tortonian ponded sheets exposed just north of the

Sierra Alhamilla closely resemble the Late Tortonian/early Messinian Alfaro sub-basin fill and may represent deposition within another but earlier transtensional depression later inverted in transpression.

Evidence for syn-depositional strike-slip deformation creating local accommodation on the sea floor in both the Tabernas and Sorbas basins is seemingly at variance with the recent focus on normal faults and regional extension in driving Late Miocene basin formation in the area (Andrić et al., 2018; Valetti et al., 2019). However, Giaconia et al. (2014) pointed to the importance of strike-slip transfer faults in areas undergoing regional heterogenous extension and showed that these bound Tortonian depocentes in the eastern Sorbas Basin. Similarly the Alpujarras Corridor (Sanz De Galdeano et al., 1985; **Figure 1**) to the west of the Tabernas Basin has been interpreted as a dextral strike-slip fault zone transferring deformation between areas undergoing different styles and amounts of Miocene to Recent extension (Martínez-Martínez, 2006). The Alfaro sub-basin lies on the eastward projection of the Alpujarras structure to link with the fault zone on the northern flank of the Alhamilla. The implication is that transtension on long transfer faults opened up local depocentres (sub-basins) distinct from the titled fault-block depocentres in the hanging wall of the main detachment faults.

Basins resembling the Alfaro sub-basin are seen today on the floor of the Alboran Sea south of the Tabernas area where they have been imaged on seismic profiles. The Alboran Basin is divided into several small sub-basins which have mainly been controlled by active right-lateral transpression due to oblique Africa-Iberia convergence since the late Tortonian (Bourgois et al., 1992; Comas et al., 1992; Woodside and Maldonado, 1992). Alvarez-Marrón (1999) interprets some of the sub-basins in the eastern Alboran Sea as negative flower structures. The Yusuf Basin is a 16 km long by 9 km wide depocentre bounded by a pair of sub-vertical faults. The dextral oblique-slip Yusuf Fault forms a master fault on the northern side of the basin. Subsidence in the basin was asymmetric wedging towards the Yusuf Fault (**Figure 1**). Subordinate faults on the south side of the basin step down into the basin. Moreover the downthrown/flexed basin margins are characterised by listric extensional faults caused by gravitational sliding.

7 CONCLUSION

Turbidite successions vary widely reflecting different combinations of up-dip supply, sea-level fluctuations and basin tectonics, as well as local factors (Reading, 1996). Tabernas turbidites are important in that they provide a rare outcrop example of a system strongly forced by changes in receiving basin morphology—in this case driven by tectonic deformation of the sea bed. A phase of syndepositional faulting and folding controlled the location and wavelength of depocentres on the floor of the basin, the stability of slopes, failure triggering, flow pathways, and switching between bypass, confined fans and ponded flows. Dextral-oblique strike-slip faults linked to form a 2 km wide transtensional sub-basin filled by an expanded section of ponded turbidite sheets. Elsewhere, flows were also ponded in synclinal fold axes. The sub-basin was asymmetric, the fill thinning and onlapping to the south, with sheet turbidites juxtaposed against the main fault zone in the north. Sub-basin topography was rapidly buried as the faults became inactive with a series of large mass-transport deposits forming as an unstable (tectonically tilted) slope created in response to the compressional uplift of the western end of the Alhamilla block. This created a dynamic onlap slope very different in character to the generally more passive onlaps described from other basins. Small fault-controlled deep-water depocentres in SE Spain and the Alboran Sea analogous to the Alfaro sub-basin were developed more widely and may have been localised on long transfer faults accommodating heterogenous extension. The well-exposed Tabernas example serves to highlight the complex interplay between tectonic deformation, flow processes and sea floor instability that can occur in deep-water sub-basins opened up on active strike-slip faults.

DATA AVAILABILITY STATEMENT

The raw data supporting the conclusion of this article will be made available by the authors, without undue reservation.

AUTHOR CONTRIBUTIONS

All authors listed have made a substantial, direct, and intellectual contribution to the work and approved it for publication.

FUNDING

ACKNOWLEDGMENTS

REFERENCES

Aksu, A. E., Calon, T. J., Hiscott, R. N., and Yasar, D. (2000). Anatomy of the North Anatolian Fault Zone in the Marmara Sea, Western Turkey: Extensional Basins above a Continental Transform. *GSA Today* 10, 3–7.

Alvarez-Marrón, J. (1999). Pliocene to Holocene Structure of the Eastern Alboran Sea (Western Mediterranean). *Proc. Ocean Drill. Program Sci. Results* 161, 345–355. doi:10.2973/odp.proc.sr.161.224.1999

Amy, L. A., McCaffrey, W. D., and Kneller, B. C. (2004). "The Influence of a Lateral basin-slope on the Depositional Patterns of Natural and Experimental Turbidity Currents," in *Deep-Water Sedimentation in the Alpine Basin of SE*

France: New Perspectives on the Grès d'Annot and Related Systems. Editors P. Joseph and S.A. Lomas. London: Geological Society, London, Special Publications, 221, 311–330. doi:10.1144/gsl.sp.2004.221.01.17

Andrić, N., Matenco, L., Hilgenand de Bresser, H. (2018). Structural Controls on Sedimentation During Asymmetric Extension: The Case of Sorbas Basin (SE Spain). Glob. Planet. Change 171, 185–206.

Augier, R., Jolivet, L., and Robin, C. (2005). Late Orogenic Doming in the Eastern Betic Cordilleras: Final Exhumation of the Nevado-Filabride Complex and its Relation to basin Genesis. Tectonics 24. doi:10.1029/2004tc001687

Barnes, P. M., Sutherland, R., Davy, B., and Delteil, J. (2001). Rapid Creation and Destruction of Sedimentary Basins on Mature Strike-Slip Faults: an Example from the Offshore Alpine Fault, New Zealand. J. Struct. Geology. 23, 1727–1739. doi:10.1016/s0191-8141(01)00044-x

Beaubouef, R. T., and Abreu, V. (2010). "MTCs of the Brazos-Trinity Slope System; Thoughts on the Sequence Stratigraphy of MTCs and Their Possible Roles in Shaping Hydrocarbon Traps," in Submarine Mass Movements and Their Consequences. Editors D. C. Mosher, R.C. Shipp, L. Moscardelli, J.D. Chaytor, C.D.P. Baxter, H.J. Lee, et al. Advances in Natural and Technological Hazards Research. Dordrecht: Springer Science, 28, 475–490. doi:10.1007/978-90-481-3071-9_39

Ben-Avraham, Z., and Zoback, M. D. (1992). Transform-normal Extension and Asymmetric Basins: An Alternative to Pull-Apart Models. Geol 20, 423–426. doi:10.1130/0091-7613(1992)020<0423:tneaab>2.3.co;2

Bradley, D., and Hanson, L. (1998). Paleoslope Analysis of Slump Folds in the Devonian Flysch of Maine. Maine. J. Geol 106, 305–318.

Bourgois, J., Mauffret, A., Ammar, A., and Demnati, A. (1992). Multichannel Seismic Data Imaging of Inversion Tectonics of the Alboran Ridge (Western Mediterranean Sea). Geo-Marine Lett. 12, 117–122. doi:10.1007/bf02084921

Bozkurt, E., and Koçyiðit, A. (1996). The Kazova basin: an Active Negative Flower Structure on the Almus Fault Zone, a Splay Fault System of the North Anatolian Fault Zone, Turkey. Tectonophysics 265, 239–254. doi:10.1016/s0040-1951(96)00045-5

Britter, R. E., and Linden, P. F. (1980). The Motion of the Front of a Gravity Current Travelling Down an Incline. J. Fluid Mech. 99, 531–543. doi:10.1017/s0022112080000754

Bull, S., Cartwright, J., and Huuse, M. (2009). A Review of Kinematic Indicators from Mass-Transport Complexes Using 3D Seismic Data. Mar. Pet. Geology. 26, 1132–1151. doi:10.1016/j.marpetgeo.2008.09.011

Catterall, V., Redfern, J., Gawthorpe, R., Hansen, D., and Thomas, M. (2010). Architectural Style and Quantification of a Submarine Channel-Levee System Located in a Structurally Complex Area: Offshore Nile Delta. J. Sediment. Res. 80, 991–1017. doi:10.2110/jsr.2010.084

Comas, M. C., García-Dueñas, V., and Jurado, M. J. (1992). Neogene Tectonic Evolution of the Alboran Sea from MCS Data. Geo-Marine Lett. 12, 157–164. doi:10.1007/bf02084927

Cunha, R. S., Tinterri, R., and Muzzi Magalhaes, P. (2017). Annot Sandstone in the Peïra Cava basin: An Example of an Asymmetric Facies Distribution in a Confined Turbidite System (SE France). Mar. Pet. Geology. 87, 60–79. doi:10.1016/j.marpetgeo.2017.04.013

Dabrio, C. J. (1990). "Fan-delta Facies Associations in the Late Neogene and Quaternary Basins of southeastern Spain," in Coarse-Grained Deltas. Editors A. Colella and D.B. Prior. Oxford: Special Publication,International Association of Sedimentologists, 10, 91–111.

De Galdeano, C. S., Rodriguez-Fernandez, J., and López-Garrido, A. C. (1985). A Strike-Slip Fault Corridor within the Alpujarra Mountains (Betic Cordilleras, Spain). Geol. Rundsch. 74, 641–655. doi:10.1007/bf01821218

De Lamotte, D. F., Guezou, J.-C., and Averbuch, O. (1995). Distinguishing Lateral Folds in Thrust-Systems; Examples from Corbières (SW France) and Betic Cordilleras (SE Spain). J. Struct. Geology 17, 233–244. doi:10.1016/0191-8141(94)e0035-w

Doughty-Jones, G., Mayall, M., and Lonergan, L. (2017). Stratigraphy, Facies, and Evolution of Deep-Water Lobe Complexes within a Salt-Controlled Intraslope Minibasin. Bulletin 101, 1879–1904. doi:10.1306/01111716046

Doyle, P., Mather, A. E., Bennett, M. R., and Bussell, M. A. (1996). Miocene Barnacle Assemblages from Southern Spain and Their

Palaeoenvironmental Significance. Lethaia 29, 267–274. doi:10.1111/j.1502-3931.1996.tb01659.x

Frey-Martínez, J., Cartwright, J., and James, D. (2006). Frontally Confined versus Frontally Emergent Submarine Landslides: A 3D Seismic Characterisation. Mar. Pet. Geology 23, 585–604. doi:10.1016/j.marpetgeo.2006.04.002

Galdeano, C. S., and Vera, J. A. (1992). Stratigraphic Record and Palaeogeographical Context of the Neogene Basins in the Betic Cordillera, Spain. Basin Res. 4, 21–36. doi:10.1111/j.1365-2117.1992.tb00040.x

Giaconia, F., Booth-Rea, G., Martínez-Martínez, J. M., Azañón, J. M., Storti, F., and Artoni, A. (2014). Heterogeneous Extension and the Role of Transfer Faults in the Development of the southeastern Betic Basins (SE Spain). Tectonics 33, 2467–2489. doi:10.1002/2014tc003681

Gray, T. E., Alexander, J., and Leeder, M. R. (2005). Quantifying Velocity and Turbulence Structure in Depositing Sustained Turbidity Currents across Breaks in Slope. Sedimentology 52, 467–488. doi:10.1111/j.1365-3091.2005.00705.x

Haughton, P. (2001). Contained Turbidites Used to Track Sea Bed Deformation and basin Migration, Sorbas Basin, South-East Spain. Basin Res. 13, 117–139. doi:10.1046/j.1365-2117.2001.00143.x

Haughton, P. D. W. (2000). Evolving Turbidite Systems on a Deforming basin Floor, Tabernas, SE Spain. Sedimentology 47, 497–518. doi:10.1046/j.1365-3091.2000.00293.x

Heiniö, P., and Davies, R. J. (2007). Knickpoint Migration in Submarine Channels in Response to Fold Growth, Western Niger Delta. Mar. Petrol. Geol. 24, 424–449. doi:10.1016/j.marpetgeo.2006.09.002

Hodgson, D. M., and Haughton, P. D. W. (2004). "Impact of Syndepositional Faulting on Gravity Current Behaviour and Deep-Water Stratigraphy: Tabernas-Sorbas Basin, SE Spain," in Confined Turbidite Systems. Editors S. A. Lomas and P. Joseph. London: Geological Society, London, Special Publications, 222, 135–158. doi:10.1144/gsl.sp.2004.222.01.08

Hodgson, D. M. (2002). Tectono-stratigraphic Evolution of a Neogene Oblique Extensional Orogenic basin, Southeast Spain. Ph.D. thesis. University of London.

Howlett, D. M., Gawthorpe, R. L., Ge, Z., Rotevatn, A., and Jackson, C. A. L. (2021). Turbidites, Topography and Tectonics: Evolution of Submarine Channel-lobe Systems in the Salt-influenced Kwanza Basin, Offshore Angola. Basin Res. 33, 1076–1110. doi:10.1111/bre.12506

Iaccarino, S., Morlotti, E., Papani, G., Pelosio, G., and Raffi, S. (1975). Lithostratigrafia e biostratigraphia di alcune serie Neogeniche della provinca di Almeria (Andalusia orientale, Spagna). Ateno Parmense, Acta Naturalia 11, 237–313.

Kleverlaan, K. (1987). Gordo Megabed: a Possible Seismite in a Tortonian Submarine Fan, Tabernas basin, Province Almeria, Southeast Spain. Sediment. Geol. 51, 181–213. doi:10.1016/0037-0738(87)90047-9

Kleverlaan, K. (1989a). Neogene History of the Tabernas basin, (SE Spain) and its Tortonian Submarine Fan Development. Geol. Mjnb. 68, 421–432.

Kleverlaan, K. (1989b). Three Distinctive Feeder-Lobe Systems within One Time Slice of the Tortonian Tabernas Fan, SE Spain. Sedimentology 36, 25–45. doi:10.1111/j.1365-3091.1989.tb00818.x

Kneller, B. (2003). The Influence of Flow Parameters on Turbidite Slope Channel Architecture. Mar. Pet. Geology 20, 901–910. doi:10.1016/j.marpetgeo.2003.03.001

Koch, H., and McCann, T. (2020). Petrological Characterisation and Provenance of the Shelf to Deep-marine Sandstones from the Neogene-Age Tabernas Basin, SE Spain. zdgg 171, 521–549. doi:10.1127/zdgg/2020/0245

Lazar, M., Ben-Avraham, Z., and Schattner, U. (2006). Formation of Sequential Basins along a Strike-Slip Fault-Geophysical Observations from the Dead Sea basin. Tectonophysics 421, 53–69. doi:10.1016/j.tecto.2006.04.007

Lonergan, L., and White, N. (1997). Origin of the Betic-Rif Mountain belt. Tectonics 16, 504–522. doi:10.1029/96tc03937

Madof, A. S., Christie-Blick, N., and Anders, M. H. (2009). Stratigraphic Controls on a Salt-Withdrawal Intraslope Minibasin, north-central Green Canyon, Gulf of Mexico: Implications for Misinterpreting Sea Level Change. Bulletin 93, 535–561. doi:10.1306/12220808082

Marini, M., Milli, S., Ravnås, R., and Moscatelli, M. (2015). A Comparative Study of Confined vs. Semi-confined Turbidite Lobes from the Lower Messinian Laga Basin (Central Apennines, Italy): Implications for Assessment of Reservoir Architecture. *Mar. Pet. Geology* 63, 142–165. doi:10.1016/j.marpetgeo.2015.02.015

Martín, J. M., Braga, J. C., and Riding, R. (1998). "Messinian Reefs and Stromatolites of the Sorbas Basin, Almería, SE Spain," in *15th IAS Field Trip Guide Book*. Editors A. Meléndez-Hevia and A.R. Soria. Alicante: Instituto Tecnologico Geominero de España,111–125.

Martínez-Martínez, J. M., and Azañón, J. M. (1997). Mode of Extensional Tectonics in the southeastern Betics (SE Spain): Implications for the Tectonic Evolution of the Peri-Alborán Orogenic System. *Tectonics* 16, 205–225. doi:10.1029/97tc00157

Martínez-Martínez, J. M., and Azañón, J. M. (2002). Orthogonal Extension in the Hinterland of the Gibraltar Arc (Beltics, SE Spain). *J. Virtual Explorer* 8, 3–22.

Martínez-Martínez, J. M. (2006). Lateral Interaction between Metamorphic Core Complexes and Less-Extended, Tilt-Block Domains: The Alpujarras Strike-Slip Transfer Fault Zone (Betics, SE Spain). *J. Struct. Geology* 28, 602–620. doi:10.1016/j.jsg.2006.01.012

Martinsen, O. (1994). "Mass Movements," in *The Geological Deformation of Sediments*. Editors A. Maltman (London: Chapman and Hall), 127–165. doi:10.1007/978-94-011-0731-0_5

Mayall, M., Lonergan, L., Bowman, A., James, S., Mills, K., Primmer, T., et al. (2010). The Response of Turbidite Slope Channels to Growth-Induced Seabed Topography. *Bulletin* 94, 1011–1030. doi:10.1306/01051009117

McArthur, A. D., Bailleul, J., Mahieux, G., Claussmann, B., Wunderlich, A., and McCaffrey, W. D. (2021). Deformation-sedimentation Feedback and the Development of Anomalously Thick Aggradational Turbidite Lobes: Outcrop and Subsurface Examples from the Hikurangi Margin, New Zealand. *J. Sedim. Res.* 91, 362–389. doi:10.2110/jsr.2020.013

McCaffrey, W., and Kneller, B. (2001). Process Controls on the Development of Stratigraphic Trap Potential on the Margins of Confined Turbidite Systems and Aids to Reservoir Evaluation. *AAPG Bull.* 85, 971–988. doi:10.1306/8626ca41-173b-11d7-8645000102c1865d

Montenat, C., Ott D'Estevou, P., De Larouziere, F. D., and Bedu, P. (1987a). Origine géodynamique des bassins Néogènes du domaine Bétique Oriental (Espagne). *Total Compagnie Française des Pétroles - Notes et Mémoires* 21, 11–49.

Montenat, C., Ott D'Estevou, P., and Masse, P. (1987b). Tectonic-sedimentary Characters of the Betic Neogene Basins Evolving in a Crustal Transcurrent Shear Zone (SE Spain). *Bull. Cent. De Rech. Explor. Prod. Elf Aquitaine* 11, 1–22.

Moscardelli, L., and Wood, L. (2008). New Classification System for Mass Transport Complexes in Offshore Trinidad. *Basin Res.* 20, 73–98. doi:10.1111/j.1365-2117.2007.00340.x

Pickering, K. T., and Corregidor, J. (2005). Mass-transport Complexes (MTCs) and Tectonic Control on basin-floor Submarine Fans, Middle Eocene, South Spanish Pyrenees. *J. Sediment. Res.* 75, 761–783. doi:10.2110/jsr.2005.062

Pickering, K. T., and Hiscott, R. N. (1985). Contained (Reflected) Turbidity Currents from the Middle Ordovician Cloridorme Formation, Quebec, Canada: an Alternative to the Antidune Hypothesis. *Sedimentology* 32, 373–394. doi:10.1111/j.1365-3091.1985.tb00518.x

Pickering, K. T., Hodgson, D. M., Platzman, E., Clark, J. D., and Stephens, C. (2001). A New Type of Bedform Produced by Backfilling Processes in a Submarine Channel, Late Miocene, Tabernas-Sorbas Basin, SE Spain. *J. Sediment. Res.* 71, 692–704. doi:10.1306/2dc40960-0e47-11d7-8643000102c1865d

Pirmez, C., Beaubouef, R. T., Friedmann, S. J., and Mohrig, D. C. (2000). "Equilibrium Profile and Baselevel in Submarine Channels: Examples from Late Pleistocene Systems and Implications for the Architecture of deepwater Reservoirs," in GCSSEPM Foundation 20th Annual Research Conference, Deep-Water Reservoirs of the World, Houston, Texas, USA, 3-6 December 2000, 782–805. doi:10.5724/gcs.00.15.0782

Pizzi, M., Whittaker, A. C., Lonergan, L., Mayall, M., and Mitchell, W. H. (2021). New Statistical Quantification of the Impact of Active Deformation on the Distribution of Submarine Channels. *Geology* 49, 926–930. doi:10.1130/g48698.1

Platt, J. P., Behr, W. M., Johanesen, K., and Williams, J. R. (2013). The Betic-Rif Arc and its Orogenic Hinterland: a Review. *Annu. Rev. Earth Planet. Sci.* 41, 313–357. doi:10.1146/annurev-earth-050212-123951

Platt, J. P., and Vissers, R. L. M. (1989). Extensional Collapse of Thickened continental Lithosphere: A Working Hypothesis for the Alboran Sea and Gibraltar Arc. *Geol.* 17, 540–543. doi:10.1130/0091-7613(1989)017<0540:ecotcl>2.3.co;2

Pohl, F., Eggenhuisen, J. T., CartignyTilston, M. J. B., Tilston, M. C., de Leeuw, J., and Hermidas, N. (2020). The Influence of a Slope Break on Turbidite Deposits: An Experimental Investigation. *Mar. Geology* 424, 106160. doi:10.1016/j.margeo.2020.106160

Poisson, A. M., Morel, J. L., Andrieux, J., Coulon, M., Wernli, R., and Guernet, C. (1999). The Origin and Development of Neogene Basins in the SE Betic Cordillera (SE Spain): a Case Study of the Tabernas-Sorbas and Huercal Overa Basins. *J. Pet. Geol.* 22, 97–114. doi:10.1111/j.1747-5457.1999.tb00461.x

PuigdefàBregas, C., Gjelberg, J., and Vaksdal, M. (2004). "The Grès d'Annot in the Annot Syncline: Outer basin-margin Onlap and Associated Soft-Sediment Deformation," in *Deep-Water Sedimentation in the Alpine Basin of SE France: New Perspectives on the Grès d'Annot and Related Systems*. Editors P. Joseph and S. A. Lomas. London: Geological Society, London, Special Publications, 221, 367–388. doi:10.1144/gsl.sp.2004.221.01.20

Reading, H. G. (1996). *Sedimentary Environments: Processes, Facies and Stratigraphy*. 3rd edn. Oxford: Blackwell Science, 688.

Sanz De Galdeano, C. (1989). Las fallas de desgarre del borde Sur de la cuenca de Sorbas-Tabernas (norte de Sierra Alhamilla, Almería, Cordilleras Béticas). *Bol. Geol. y Min.* 101, 73–85.

Sanz De Galdeano, C., Shanov, S., Galindo-Zaldívar, J., Radulov, A., and Nikolov, G. (2010). A New Tectonic Discontinuity in the Betic Cordillera Deduced from Active Tectonics and Seismicity in the Tabernas Basin. *J. Geodynamics* 50, 57–66. doi:10.1016/j.jog.2010.02.005

Sinclair, H. D. (2000). Delta-fed Turbidites Infilling Topographically Complex Basins: A New Depositional Model for the Annot Sandstones, SE France. *J. Sediment. Res.* 70, 504–519. doi:10.1306/2dc40923-0e47-11d7-8643000102c1865d

Smith, R., and Joseph, P. (2004). "Onlap Stratal Architectures in the Grès d'Annot: Geometric Models and Controlling Factors," in *Deep-Water Sedimentation in the Alpine Basin of SE France: New Perspectives on the Grès d'Annot and Related Systems*. Editors P. Joseph and S. A. Lomas. London: Geological Society, London, Special Publications, 221, 389–399. doi:10.1144/gsl.sp.2004.221.01.21

Spychala, Y. T., Hodgson, D. M., Flint, S. S., and Mountney, N. P. (2015). Constraining the Sedimentology and Stratigraphy of Submarine Intraslope Lobe Deposits Using Exhumed Examples from the Karoo Basin, South Africa. *Sediment. Geology* 322, 67–81. doi:10.1016/j.sedgeo.2015.03.013

Stevenson, C. J., Talling, P. J., Wynn, R. B., Masson, D. G., Hunt, J. E., Frenz, M., et al. (2013). The Flows that Left No Trace: Very Large-Volume Turbidity Currents that Bypassed Sediment through Submarine Channels without Eroding the Sea Floor. *Mar. Pet. Geology* 41, 186–205. doi:10.1016/j.marpetgeo.2012.02.008

Tek, D. E., Poyatos-Moré, M., Patacci, M., McArthur, A. D., Colombera, L., Cullen, T. M., et al. (2020). Syndepositional Tectonics and Mass-Transport Deposits Control Channelized, Bathymetrically Complex Deep-Water Systems (Aínsa Depocenter, Spain). *J. Sedim. Res.* 90, 729–762. doi:10.2110/jsr.2020.38

Tinterri, R., Laporta, M., and Ogata, K. (2017). Asymmetrical Cross-Current Turbidite Facies Tract in a Structurally-Confined Mini-basin (Priabonian-Rupelian, Ranzano Sandstone, Northern Apennines, Italy). *Sed. Geol.* 352, 63–87. doi:10.1016/j.sedgeo.2016.12.005

Tinterri, R., and Muzzi Magalhaes, P. (2011). Synsedimentary Structural Control on Foredeep Turbidites: An Example from Miocene Marnoso-Arenacea Formation, Northern Apennines, Italy. *Mar. Petrol. Geol.* 28, 629657. doi:10.1016/j.marpetgeo.2010.07.007

Tinterri, R., and Piazza, A. (2019). Turbidites Facies Response to the Morphological Confinement of a Foredeep (Cervarola Sandstones Formation, Miocene, Northern Apennines, Italy). *Sedimentology* 66, 636–674. doi:10.1111/sed.12501

Tinterri, R., and Tagliaferri, A. (2015). "The Syntectonic Evolution of Foredeep Turbidites Related to basin Segmentation: Facies Response to the Increase in Tectonic Confinement (Marnoso-Arenacea Formation, Miocene, Northern Apennines, Italy). *Mar. Pet. Geology* 67, 81–110. doi:10.1016/j.marpetgeo.2015.04.006

Tomasso, M., and Sinclair, H. D. (2004). "Deep-water Sedimentation on an Evolving Fault-Block: the Braux and St Benoit Outcrops of the Grès d'Annot," in *Deep-Water Sedimentation in the Alpine Basin of SE France: New Perspectives on the Grès d'Annot and Related Systems.* Editors P. Joseph and S. A. Lomas. London: Geological Society, London, Special Publications, 221, 267–283. doi:10.1144/gsl.sp.2004.221.01.14

Valetti, L., Rutter, E., McCabe, A., and Mecklenburgh, J. (2019). On the Structure and Evolution of the Sorbas basin, S.E. Spain. *Tectonophysics* 773, 228230. doi:10.1016/j.tecto.2019.228230

Vissers, R. L. M., Platt, J. P., and Van Der Wal, D. (1995). Late Orogenic Extension of the Betic Cordillera and the Alboran Domain: a Lithospheric View. *Tectonics* 14, 786–803. doi:10.1029/95tc00086

Weijermars, R., Roep, T. H. B., Van Den Eeckhout, B., Postma, G., and Kleverlaan, K. (1985). Uplift History of a Betic Fold Nappe Inferred from the Neogene-Quaternary Sedimentation and Tectonics (In the Sierra Alhamilla and Almería, Sorbas and Tabernas Basins of the Betic Cordillera, SE Spain). *Geol. Mijnb.* 64, 379–411.

Wood, R. A., Pettinga, J. R., Bannister, S., Lamarche, G., and McMorran, T. J. (1994). Structure of the Hanmer Strike-Slip basin, Hope Fault, New Zealand. *Geol.Soc.Am.Bull.* 106, 1459–1473. doi:10.1130/0016-7606(1994)106<1459:sothss>2.3.co;2

Woodside, J. M., and Maldonado, A. (1992). Styles of Compressional Neotectonics in the Eastern Alboran Sea. *Geo-Marine Lett.* 12, 111–116. doi:10.1007/bf02084920